Mapping epilepsy-specific functional MRI network properties in refractory epilepsy using intracranial EEG locations

Sediqa Amin

A thesis submitted to

Auckland University of Technology

in partial fulfilment of the requirements for the degree of Master of Philosophy

2025

Department of Psychology and Neuroscience

Faculty of Health and Environmental Sciences

Supervisor: Associate Professor Mangor Pedersen

Abstract

Epilepsy is a heterogeneous neurological disorder characterized by sudden and unpredictable seizures that disrupt normal brain function. Globally, about 5 million people are diagnosed with epilepsy each year, which makes up a significant portion of the world's disease burden. Epilepsy is increasingly considered a brain network disorder whereby seizure activity in one region of the brain affects the neuronal activity in other brain regions in the network, which means that brain networks are involved in seizure generation and propagation. Brain interactions are known to be dynamic, even in a resting state; therefore, the functional connectivity (FC) of brain regions analysed in fMRI data also varies over time. This thesis aims to study alteration in local dynamic functional connectivity in the regions of interest in the ipsilateral hemisphere (hemisphere where seizures originates), by comparing them to the homologous hemispheric areas. This was done by using the presurgical intracranial electroencephalograpgy (iEEG) electrode implantation as a locator of the presumed epileptogenic zone with rapid functional MRI (fMRI – 608 ms per image) data for dynamic functional connectivity analysis in 17 patients with drug-resistant epilepsy. Dynamic functional connectivity was computed using the dynamic regional phase synchrony (DRePS) method. A comparative analysis using the standard deviation (i.e., variability) of DRePS showed significant temporal variability in ipsilateral regions in 6 out of 17 epilepsy patients. Four showed decreased variability, and 2 showed increased temporal variability in the ipsilateral areas. This indicates an alteration in dynamic functional connectivity in the region of interest in the disease hemisphere. However, non-significant temporal alteration in other subjects might indicate more global network alteration due to disease progression. Large-scale ventricular brain abnormality was also observed in 3 subjects, rendering it challenging to estimate contralateral brain regions in these cases analytically. Understanding the effects of seizure activity on functional connectivity and analysing the properties of network topology can help in further pathological studies and surgical planning in drug-resistant focal epilepsy.

Contents

List of Figures

List of Tables

List of Appendix Figures

Attestation of Authorship

I affirm that this submission is my original work and to the best of my knowledge it does not include materials previously published or authored by others (unless clearly acknowledged). Furthermore, artificial intelligence or generative artificial intelligence tools were not used unless clearly stated, referenced, and accompanied by their intended purpose. Additionally, this work has not been submitted for any other academic degree or diploma from any university or institution of higher education.

Signature Date: 01 May 2025

Acknowledgements

I would like to take this opportunity to express my gratitude to a few remarkable people who have supported me and whom I had the honor of knowing and working with.

First of all, I would like to thank my family members, especially my mother, who supported me and encouraged me in pursuing my passion.

I extend my heartfelt gratitude to my supervisor, Associate Professor Mangor Pedersen, for his unwavering support and guidance throughout this journey. His mentorship has been invaluable as he patiently corrected my mistakes, shared his profound knowledge on the subject, and provided clarity whenever needed. Our brainstorm sessions were always incredibly productive and crucial to advancing my work. Thank you, Mangor, for your enduring encouragement and dedication.

I would like to extend my warm regards to participants who participated in this rare intracranial EEG recording and functional magnetic resonance imaging study. I also wish to acknowledge the Utrecht Medical Center for their efforts in collecting and uploading the iEEG and fMRI data on the OpenNeuro platform, making it accessible for clinical research. My sincere appreciation goes to the OpenNeuro team for providing an invaluable online resource of neuroimaging data to support further research endeavors.

Ethics Approval

The ethical approval for this research was not required as the de-identified dataset of intracranial EEG recordings and fMRI images of people with epilepsy was retrieved online at https://openneuro.org/datasets/ds003688. The data collection was approved by the Medical Ethical Committee of the Utrecht University Medical Center in compliance with the Declaration of Helsinki (2013) and uploaded on OpenNeuro which is an open-access repository for neuroimaging data (Berezutskaya et al., 2022). All datasets available on OpenNeuro are shared under the Creative Commons CC0 license allowing its ethical and unrestricted use in scientific research. Ethical approval for the use of these datasets was provided by the original authors of the datasets adhering to all relevant privacy and regulations of OpenNeuro. All the datasets have been de-identified to ensure the protection of participants' personal health information (Neuroscience, 2015-2025).

Chapter 1 Literature review

1.1 Background

Epilepsy is a chronic neurological disorder affecting all genders, races, and age groups. Globally around 50 million people are affected by epilepsy, which makes up a significant proportion of the population with chronic disease. The estimated proportion of active epileptic patients is 4 to 10 per 1000 individuals at a given time (World Health Organization, 2024). Approximately one-third of epileptic patients are diagnosed with refractory epilepsy (i.e., seizures are not controlled by antiepileptic drug (Stafstrom & Carmant, 2015). In New Zealand, about 45,000-50,000 people are currently living with epilepsy which make up about 1% to 2% of the population of New Zealand (Neurological Foundation, 2019). Epilepsy is 40% more common in Māori children than in other ethnicities in New Zealand (Health Research Council of New Zealand). According to the International League Against Epilepsy (ILAE) and the International Bureau for Epilepsy (IBE), Epilepsy is defined as "a disorder of the brain characterized by an enduring predisposition to generate epileptic seizures and by the neurobiological, cognitive, psychological, and social consequences of this condition" (Fisher et al., 2005, p. 471). Epileptic seizure can be defined as distortion in the electrical activity of a neuronal network in the brain, causing events of paroxysmal behaviours and movements and altering levels of consciousness. Seizures onset can occur in the cortical or subcortical structures of the brain (Giourou et al., 2015).

1.2 Types of epilepsy

The ILAE has categorized epilepsy into three groups based on the type of seizure onset. These include focal, generalized, and unknown types of epilepsy (Fisher et al., 2017). This classification is based on neurophysiological and neuroanatomical data of complex brain networks (San-Juan & Rodríguez-Méndez, 2023). In focal epilepsy, seizures are limited to one hemisphere, whereas in generalized epilepsy seizures originate and distribute in a bilateral hemispheric neuronal network (Sirven, 2015).

1.2.1 Focal epilepsy

The seizure affecting a single region of the brain causes focal epilepsy (Fisher et al., 2017). The signs and symptoms of focal epilepsy depend on the region of the brain involved. Such as, seizure onset occurring at the occipital lobe causes visual phenomena, precentral gyrus causes rhythmic tonic or clonic motor symptoms, and postcentral gyrus with sensory dysfunction such as paresthesias (Stafstrom & Carmant, 2015). Focal seizure is classified as focal aware (previously known as simple partial seizure when the patient is aware of symptoms during a seizure) and as focal impaired awareness (formerly known as complex partial seizure where the patient's consciousness is impaired and is not able to respond to external stimuli during a seizure). Focal impaired awareness occurs due to seizure onset in the temporal lobes (Fisher et al., 2017).

In focal epilepsy, the functional anatomy of seizure provides details of complex networks involving seizure initiation and spread comprising four components.

1. Seizure focus: The seizure focus is the starting point of a seizure where the physiological spark of seizure begins. It is not a single site but a region with multiple independent points that can initiate seizures, known as multifocality. This is supported by intracranial electroencephalographic recordings, which shows that seizures with different clinical features can originate from distinct patterns within the same seizure onset zone. In mesial temporal lobe epilepsy for example, seizures may have a broad synchronized onset across multiple limbic structures or arise independently from different sites. This shift in understanding moves away from the idea of a single synchronized seizure focus only to a more complex multifocal model.
2. Initiating circuit: The initial circuit is a network of interconnected brain regions that amplifies the spark from seizure focus and sustains it by transforming it into active seizure dynamics. While the seizure focus is an initial spark, emerging evidence suggests that a broader network is essential to support, organize, and sustain seizure activity.
3. Pathways of spread: The pathways of seizure spread are specific routes through which seizure expands beyond the initiating circuit, recruiting additional brain regions. These patterns are highly stereotyped in individuals and play a key role

in the secondary generalization of seizures. At the same time, various theories have been proposed to explain how seizures propagate. These include seizure-induced changes in the extracellular environment, the strength of existing pathways i.e., local, regional, or subcortical, and the inherent susceptibility of certain regions to seizure activity.

4. Modulatory centers: The modulatory centers are regions outside the initiating circuit or pathways of spread that influence the seizure threshold, affecting easily how a seizure can occur by altering its excitability and the likelihood of seizure initiation or propagation. While not directly involved in early seizure activity, these centers play an essential role in modulating clinical outcomes, as evidenced by variability in seizure intensity and duration. The diverse clinical presentations within the same individual, ranging from non-convulsive episodes to full tonic-clonic events, underscore the dynamic influence of neuromodulatory centers. Although these regions may not directly participate in electrographic seizure activity, they are integral to the functional anatomy of seizure circuits, shaping the probability and progression of seizures.

This framework highlights how seizures progress from localized origins to widespread brain activity (Bertram, 2013).

1.2.2 Generalized epilepsy

In generalized epilepsy, the seizures spread to other regions of the brain, affecting globally (Fisher et al., 2017). Generalized seizures are classified into Absence, generalized tonic-clonic, myoclonic, and atonic seizures. Absence (petit mal) involves sudden and brief loss of consciousness and unresponsiveness. Other symptoms include eye blinking and head nodding. Generalized tonic-clonic or grand mal seizures cause bilateral symmetric tonic (stiffening) movements followed by clonic (rhythmic jerking) movements and impaired consciousness. Myoclonic seizure is brief involuntary muscle movements or jerks without any sign of lapse in consciousness. Myoclonic jerks are regularly not repetitive and can be focal or generalized. Atonic seizure causes loss of tone in body muscles, resulting in a head drop or fall to the ground (Stafstrom & Carmant, 2015).

1.2.3 Unknown

In the unknown type of epilepsy, seizures cannot be categorized as either generalized or focal (Shariff et al., 2024). The seizures of unknown onset can be classified into motor and non-motor. These include tonic-clonic, epileptic spasms, and behavioral arrests (Fisher et al., 2017). Epileptic spasms involve brief (few seconds) and sudden extension and flexion of arms and legs, which occur in clusters. Epileptic spasms that appear at the first year of age are called infantile spasms (west syndrome); however, epileptic spasms can affect any age group (Stafstrom & Carmant, 2015).

1.3 Etiology

It is crucial to determine the disease etiology for appropriate management and treatment of epileptic patients. Based on its underlying cause or origin, epilepsy is classified into the following sub-groups.

1.3.1 Structural

The concept of structural etiology is defined as structural brain abnormalities linked to an increased risk of epilepsy. These structural brain abnormalities are visible in neuroimaging. Structural abnormalities can be genetic, such as cortical malformations, or acquired, e.g., stroke, trauma, or infections.

1.3.2 Genetic

Genetic etiology means that presumed genetic mutations cause epileptic seizures. These can be inherited or de novo mutations. The genetic etiology of epilepsy is diverse, and in most cases, the causal genes are still unknown. Epilepsies that are categorized under genetic etiology are based on three points. First, it can be based on the family history of patients. Second, it can be based on clinical research of epilepsies among populations having the same syndrome e.g., Juvenile Myoclonic Epilepsy. Third, it includes the study of the molecular basis of epilepsy. Such as the identification of genetic variants associated with the phenotype of epilepsy.

1.3.3 Infectious

Globally the most common cause of epilepsy is infections in the central nervous system. This includes epilepsy caused by unknown acute infections such as meningitis or

encephalitis. Infectious etiology also includes the postinfectious development of epilepsy.

1.3.4 Metabolic

There is a wide range of epilepsies that are associated with metabolic disorders. Epilepsies that are caused by presumed or unknown metabolic disorders are categorized in metabolic etiology, such as aminoacidopathies or pyridoxine-dependent seizures.

1.3.5 Immune

Epilepsies caused by immune disorders where autoimmune-mediated inflammations occur in the central nervous system are categorized in immune etiology, e.g., autoimmune encephalitis like anti-NMDA receptor encephalitis.

1.3.6 Unknown

There are certain epilepsies where the cause of the disease is still unknown despite thorough investigation (Scheffer et al., 2017).

1.4 Epileptogenesis

The process in which normal brain tissue becomes capable of seizure generation and progression is known as epileptogenesis (Chen et al., 2021). During epileptogenesis, changes at cellular and molecular levels such as genetic, membrane channels, intracellular signaling pathways, neurotransmission, and synaptic connectivity occur. These changes cause hyperexcitability and hypersynchrony permanently in the brain. The study of the mechanism of epileptogenesis has become a focus of research to avert seizures' physiological, behavioral, and cognitive effects on the human brain (Stafstrom, 2006).

1.4.1 Hyperexcitability and hypersynchrony

Hyperexcitability and hypersynchrony are considered the hallmarks of seizure in neuronal networks. Hypersynchrony refers to the firing of the action potential of a group of neurons simultaneously and at the same rate. Hyperexcitability is when a threshold of excitation in neuronal circuits exceeds the limits, causing seizure generation as depicted in figure 1.2. Excessive excitation, reduced inhibition, or both regulate the seizure generation, propagation, and termination. This can occur in any region of the

brain. Therefore, understanding the process of excitation and inhibition in seizure generation makes potential drug targets (Stafstrom, 2006). There are several causes of hyperexcitability.

- The hyperexcitability of neurons can be intrinsic. These include types, numbers, and opening and closing of voltage-gated ion channels such as sodium or potassium. The alterations in these ion channels can occur during gene expression, post-translational modification, or through second messengers.
- The extrinsic factors causing hyperexcitability include abnormal ion concentrations within cells and changes in the metabolism of extracellular neurotransmitters or uptake by glial cells.
- Alterations of synaptic neurotransmitters can cause local seizures. These include an increase in excitatory signalling, such as glutamate or a decrease in inhibitory signalling such as GABA (gamma-aminobutyric acid) in the synapse of neurons given in figure 1.1. Gene expression alterations of transmembrane-gated ionotropic channels, changes in synapse configuration and gap-junction synaptic function also cause hyperexcitability.

Figure 1-1

A simplified overview of imbalance in excitation and inhibition leading to epileptic seizures.

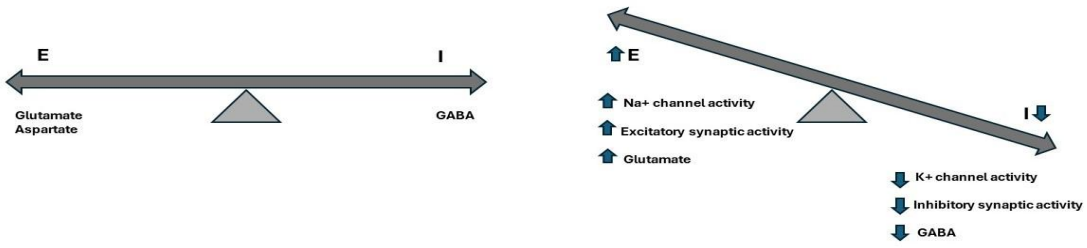

Compared to normal excitation/inhibition, in epilepsy, the imbalance of excitatory/inhibitory factors such as ion channel activity, excitatory/inhibitory synaptic activity, and neurotransmitters, causes seizure initiation.

The key elements of epileptogenesis are the imbalance of excitation/inhibition and modifications in neural communication, which causes neuronal population synchrony.

Figure 1-2

Depicting action potential and abnormal epileptic discharge.

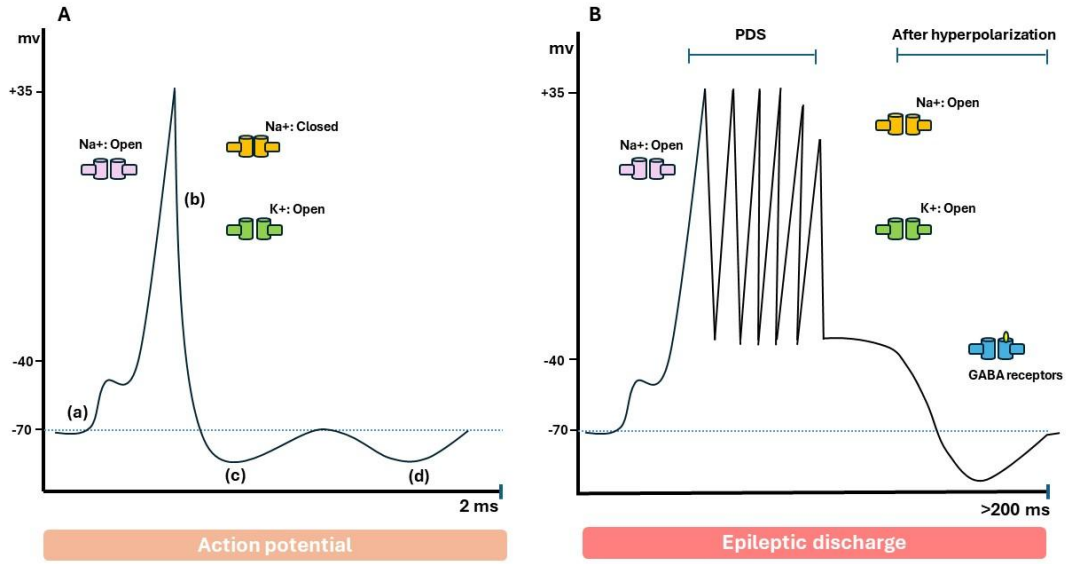

Action potential of a neuron (a) excitatory postsynaptic potential, (b) action potential mediated by sodium channel, (c) hyperpolarization AHP, its duration and magnitude determine the next action potential, (d) inhibitory postsynaptic potential PSP caused by activation of inhibition. The ion balance is restored by membrane Na+, K+ channels and glial cells. (B) Blockage of (d) results in expression of NMDA receptor channel mediated Ca+ spikes and paroxysmal depolarization shift.

In both focal and generalized epilepsies, the excitation is increased similarly but differs in the synchronisation mechanism (Giourou et al., 2015). Focal seizures originate within a neuronal network and spread to one hemisphere only (Nascimento et al., 2023). The basic mechanism of focal seizure involves the imbalance of excitation and inhibition in neurons. The inhibitory interneurons are suggested to be the basis of cellular processes that cause large-scale discharges in seizure initiation. After the intense activation of inhibitory interneurons, the temporarily silenced excitatory cells produce recurrent discharges and fast oscillations that mark the seizure onset zone. It is suggested that the seizure onset zone consists of microdomains that exhibit high-frequency firing, causing microseizures. These microdomains merge into larger domains, causing ictal transmission and macroseizure. The synchronization pattern evolves in the seizure from early ictal desynchronization to large-scale synchronization. On network level seizures

reflect multi-scale phenomena disrupting brain networks. Therefore, long-term repetitive seizures can permanently alter cortical networks, leading to spontaneous recurrences (Giourou et al., 2015). Understanding typical absence seizures driven by thalamocortical circuitry provides key insights into the mechanisms underlying generalized epilepsies.

Contrary to earlier studies, it is now suggested that all seizures, even those of generalized seizures originate in local microcircuits and propagate from an initial ictogenic zone. The prototype epileptic circuit suggests that generalized seizures begin at neocortical focus interacting with thalamocortical neurons and activating GABAergic neurons (that release inhibitory neurotransmitter Gamma-aminobutyric acid GABA) within the reticular thalamic nucleus. This interaction triggers oscillatory activity spreading throughout cortical networks culminating in synchronized EEG rhythms. For instance, “frontal absences” are thought to result from rapid secondary generalization by a frontal focus (Chang & Lowenstein, 2003; Giourou et al., 2015).

1.4.2 Epileptogenic zone

The epileptogenic zone is defined as an “area of cortex that is necessary and sufficient for initiating seizures and whose removal (or disconnection) is necessary for complete abolition of seizures”. For preoperative assessment purposes five cortical zones are proposed.

- Irritative zone is an area of the brain that generates interictal epileptiform spikes in electrography.
- Seizure onset zone is a cortical region of the brain where seizures initiate.
- Symptomatogenic zone is the area of the brain that, when activated by epileptic seizure, produces initial ictal symptoms.
- Epileptogenic lesion is an area of the brain where the lesion itself or by secondary hyperexcitability leads to an epileptic seizure.
- Functional deficit zone is the cortical region of the brain that cannot function properly during interictal period (San-Juan & Rodríguez-Méndez, 2023). The figure 1.3 shows overlap of cortical zones in epilepsy.

Figure 1-3

Diagrammatic representation of overlap of cortical zones of epilepsy.

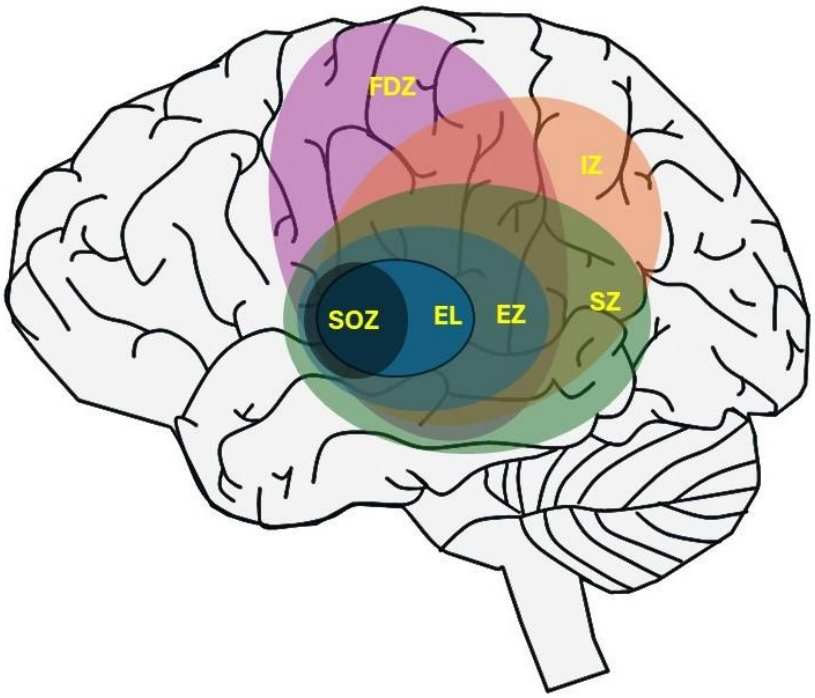

SOZ is seizure onset zone. EL is epileptogenic lesion. EZ is epileptogenic zone. SZ is symptomatogenic onset zone. IZ is the irritative zone and FDZ is functional deficit zone.

1.5 Refractory epilepsy

Refractory epilepsy also known as drug-resistant epilepsy is established when antiepileptic drugs (AEDs) fail to control seizures (Beleza, 2009). Approximately 30% to 40% of epilepsies are refractory epilepsy. According to International League Against Epilepsy (ILAE) drug-resistant epilepsy is defined as "failure of adequate trial of two tolerated, appropriately chosen, and unused antiepileptic drug schedules (whether as monotherapies or in combination) to achieve sustained seizure freedom" (Engel Jr, 2014, p. S13). Risk factors associated with refractory epilepsy identified by Beleza (2009) include the following.

- Epileptic patients with lesions, hippocampal sclerosis, cortical dysplasia, and hemorrhages are more likely to develop refractory epilepsy.

- High frequency of seizures.
- High frequency of interictal and multifocal spikes in electroencephalography.
- Inadequate response to first 2 AEDs.
- Early epilepsy onset .

Treatment options for Treatment options for refractory epilepsy include AED optimization, non-surgical and surgical interventions, and complementary and alternative medicines. Surgical treatment depends on the type of epilepsy and its etiology. This includes curative resection, such as temporal lobectomy, vagus nerve stimulation, callosal sectioning, and multiple subpial transection (Bacon et al., 2023; Beleza, 2009). Similarly, in this study the data of patients with refractory epilepsy with given treatment options is used.

1.6 Brain network connectivity

The human brain is anatomically and functionally organized into an intricate network allowing segregation (activation of specific regions of brain) and integration (synchronized activation of large number of groups of neurons distributed across cortical regions of brain) of information (Guye, Bartolomei, & Ranjeva, 2008; Sakkalis, 2011). There has been growing interest in investigation of functional regions of brain and its interaction in normal and pathological brain. Brain connectivity mapping allows identification of active areas in the brain and involves understanding functional interactions and their localization. Brain connectivity is further divided into the following.

- Structural or neuroanatomical connectivity refers to the network of anatomical pathways tracking links between different brain regions. Magnetic resonance imaging (MRI) and diffusion tensor imaging (DTI) are used for structural connectivity analysis, providing information about white matter fibre.
- Functional connectivity refers to the statistically significant dependency patterns of activation between distant brain regions. In other words it reflects coordinated activity and communication of complex neural networks in the brain. Functional connectivity can be analysed by using local field potential LFP, electroencephalography EEEG, MEG, PET and fMRI.

- Effective connectivity is defined as the direct or indirect influence of one neural system over another at a synaptic or population level. Effective connectivity can be analyzed either directly by data-driven techniques or by model-based methods to record the activities of different brain regions (Friston, 2011; Sakkalis, 2011).

Based on spatial resolution, brain connectivity can be analyzed on macroscopic i.e., whole brain, mesoscopic i.e., neuronal population and microscopic meaning single neuron levels (Pedersen & Omidvarnia, 2016). The studies of human brain as a network are motivated by the concept that brain functions do not entirely reflect individual regions and connections but appear from the topology of a comprehensive neuronal network of the whole brain, that is, the connectome of the brain (van den Heuvel & Sporns, 2011). This has led to a better understanding neurological diseases such as epilepsy (Lehnertz, Brohl, & Wrede, 2023). It has been observed that some regions of the brain play an important role in global organizations characterized by their high connectivity and centrality, low clustering, and short path length, which are identified as brain hubs. Studies conducted by van den Heuvel and Sporns suggest that brain hubs have a strong tendency for mutual connection, making a central rich club which is a focal point for global communication in the brain (van den Heuvel & Sporns, 2011). Rich-club is formed by a set of brain hub. A subnetwork of rich-club is more densely connected than a random network in the brain (Kim & Min, 2020). The Diffusion magnetic resonance imaging of human subjects has shown the superior parietal and superior frontal cortex, precuneus, putamen, and thalamus as regions of rich-club in the brain (van den Heuvel & Sporns, 2011). Approximately 70% of information flow occurs by small proportion i.e., 20% of neurons which form information rich-subset in the brain. These rich club neurons have a higher firing rate than non-rich neurons (Pedersen & Omidvarnia, 2016). It is suggested that neurological disorders that affect rich-club organization deteriorate global network communication, affecting multiple brain cognitive regions (van den Heuvel & Sporns, 2011).

1.6.1 Epilepsy as network connectivity disease

Epilepsy is considered a neural network connectivity disorder (Spencer, 2002). Epileptogenic network refers to the group of interconnected regions of the brain involved in the generation and propagation of epileptic activities (Bartolomei et al.,

2017). The neuroimaging techniques such as MRI, CT, and positron emission tomography and neurophysiological assessment such as electroencephalography, transcranial magnetic stimulation, and magnetoencephalography are used for the structural and functional analysis of epileptogenic networks. Epileptogenic network analysis plays an important role in therapeutic purposes, including deep brain stimulation and vagus nerve stimulation, identifying the epileptogenic zone in the anatomical region, including epilepsy surgery. These studies identify epileptogenic areas by evaluating ictal and interictal states of epilepsy (San-Juan & Rodríguez-Méndez, 2023). EEG and neuroimaging analysis represents promising tools for studying epileptogenic activity, among other techniques (Chen et al., 2021).

1.6.2 Functional magnetic resonance imaging (fMRI)

MRI is ideal for neuronal connectivity analysis among other neuroimaging modalities due to its accessibility and translatability (Chen et al., 2021). Functional MRI is a neuroimaging tool to analyze the physiological and metabolic consequences of epileptogenesis in the brain. Compared to positron emission tomography (PET), fMRI can be used repeatedly because it lacks ionization radiation. To map electrical activity in the brain, fMRI has a high spatial resolution of a few millimeters and temporal resolution of a few seconds, while EEG and magnetoencephalography have a high temporal resolution of 10-100 milliseconds but poor spatial resolution of 1 to several centimeters. Therefore, for analysing epileptogenic zone, fMRI is considered suitable technique where EEG or PET sometimes may become inconclusive . (Kesavadas & Thomas, 2008). Functional MRI has been primarily used to localize regions of the brain activated in response to cognitive or sensory-motor tasks. fMRI has a variety of applications in clinical studies of neurological disorders, including disease mechanisms, pre-surgical evaluation of brain tumors and refractory patients, and functional analysis of the normal brain. fMRI is also used for functional analysis of regional changes in the brain related to ictal and interictal states (Detre, 2004; Kesavadas & Thomas, 2008).

1.6.2.1 fMRI methodology

In fMRI scanning brain tissue contrast is attributed to blood flow and /or metabolism. These are BOLD (blood oxygenation level-dependent) contrast and perfusion contrast. In Perfusion fMRI, arterial spin labeling (Sirin et al.) uses magnetically labeled arterial

blood water as an endogenous flow tracer. The BOLD fMRI method detects localized changes in blood oxygenation and blood flow in the brain. The BOLD fMRI method is a widely used for imaging regional brain activation because of its high signal-to-noise ratio (Detre, 2004).

The BOLD fMRI technique depends on the complex interaction of hemoglobin oxygenation, blood flow, and blood volume. During neuronal stimuli activation, oxygen consumption of functional regions of the brain increases. The ferrous iron on hemoglobin gets paramagnetic when it is de-oxygenated, which produces inhomogeneity in MRI's measurable range, causing a signal decrease in susceptibility-weighted MRI sequences (T2). During regional brain activation, oxygen consumption increases resulting in an initial decrease in deoxyhemoglobin. This causes an increase in cerebral blood flow (CBF) resulting in exceeded oxygenated hemoglobin. T2-weighted sequences detect these changes in functional regions of the brain. The signal changes of task-specific BOLD fMRI measurements are based on statistical significance level as these changes are not quantifiable in physiological units (Detre, 2004; Kesavadas & Thomas, 2008).

The fMRI also helps identify the eloquent cortex by mapping the brain's language, memory, and visual and sensorimotor control regions in presurgical epileptic patients. Thus, fMRI can define the boundary of a brain lesion and predict post-operative malfunctions of the brain's functional areas (Kesavadas & Thomas, 2008). Kesavadas et al. performed eloquent mapping in focal epilepsy and cortical malformations using fMRI. The study showed that the fMRI was the most useful method for eloquent mapping in patients with gliosis, where the gliotic lesions make predicting the eloquent cortex extremely difficult. However, the prediction of functional reorganization was unpredictable in cortical malformations (Kesavadas et al., 2007). In addition to mapping the eloquent cortex, fMRI can also be used to localize epileptogenic regions in the brain by detecting ictal and interictal activity (Detre, 2004). Earlier analysis of clinical seizures using fMRI showed significant correlations of transient focal activation with clinically determined seizure foci (Detre et al., 1995). Another study showed that EEG-fMRI is a useful method for identifying seizure foci in presumed multifocal seizure in drug-resistant epilepsy (Zijlmans et al., 2007).

Using concurrent EEG-fMRI has made localization of regional metabolic changes and ictal activity possible. This non-invasive technique capitalizes both EEG's temporal resolution and fMRI's spatial resolution in seizure localization. However, determining electrophysiological correlation was extremely difficult using EEG-fMRI concurrently. EEG-induced signal distortions in fMRI were also observed. Later, fMRI-induced EEG recording artifacts were removed by using high-resolution digitization and post-processing tools (Detre, 2004; Kesavadas & Thomas, 2008). Compared to scalp EEG, the intracranial EEG recording can detect more precise features of regional electrophysiological changes in the brain. For the sensitivity and specificity of spatial resolution intracranial EEG and fMRI, iEEG-fMRI became an ideal method after addressing safety and data quality concerns (Abreu, Leal, & Figueiredo, 2018).

1.6.3 Electrophysiological monitoring and pre-surgical assessment of refractory epilepsy

Electrophysiological recordings such as EEG are the most common and inexpensive method used for the diagnosis and management of epilepsy. EEG records the electrical activity of the neuronal population by electrodes placed on the scalp that reflect the electrical potential in apical dendrites of pyramidal cells of the cortex (Smith, 2005). EEG can record electrical activity when pyramidal cells have the same orientation and polarity and when cells are activated synchronously. The electrical potential detected by EEG is the summation of dipoles by thousands of neurons (Bromfield, Cavazos, & Sirve, 2006). The EEG recordings also provide details about the patterns of seizure and location of epileptogenic zone (San-Juan & Rodríguez-Méndez, 2023). The abnormal patterns of seizures can be distinguished by pre-ictal (changes in EEG recording preceding seizure) and ictal (changes in EEG recording during the seizure). EEG recordings can also detect electrophysiological changes in the interictal stage (the stage between two seizures) which can happen in many cases (Acharya et al., 2013). A thorough analysis of interictal events helps us understand seizure types in epilepsy. Epileptic patients show IEDs in EEG, these include spike waves, sharp waves, benign epileptiform discharges in children, spike-wave complexes, slow spike-wave complexes, 3-Hz spike-wave complexes, polyspikes, hypsarrhythmia, seizure patterns, status patterns

Intracranial EEG (iEEG) is a clinical tool measuring EEG data before/while epilepsy patients undergo remedial surgery. In drug-resistant epilepsy, surgery is the most effective treatment method. The pre-surgical assessment of the patient includes non-invasive data including ictal and interictal EEG recordings and seizure semiology. The purpose of pre-surgical assessments explained by Shah and Mittal (2014) and Smith (2005) is for confirmation of presence of epileptogenic seizure and the data is concordant with other neuroimaging data, demonstration of pathology of epileptogenicity of refracoty epileptic patient and identification of functional areas of cortex such and elquent cortex.

iEEG allows for mapping of epileptogenic biomarkers providing information about pathophysiological processes of the brain (Bartolomei et al., 2017). iEEG is considered a standard method used for the localization of epileptogenic zone and its boundary in drug-resistant epilepsy when non-invasive data are inconclusive for surgery (Jobst et al., 2020). It is an invasive method using intracranial electrodes surgically, either by placing electrodes directly on the exposed surface of the brain (i.e., subdural grid and strip electrodes) or by inserting electrodes into the parenchyma or within a lesion of the brain (Shah & Mittal, 2014). It also maps the eloquent cortex to understand its relationship to the epileptogenic zone and predict cognitive and motor functions after surgery (Jobst et al., 2020).

Subdural grid and/or depth electrodes are usually used for iEEG recordings. The subdural strip electrode consists of a configuration of electrodes (small metal discs embedded in a sheath connected to a thin insulated metal wire) in a column. When these electrodes are in rows and columns, they are known as subdural grid electrodes (Shah & Mittal, 2014). The subdural grid electrodes are used for large cortical regions for optimal coverage of cortex. However, these electrodes do not cover gray matter of the brain, cannot record seizures of deep structures, and give a poor 3D representation of the brain (Jobst et al., 2020). When a hollow plastic tube with electrodes placed inside brain tissue is called a depth electrode. Depth electrodes can be inserted in deep structures such as the hippocampus, amygdala, and brain insula (Shah & Mittal, 2014).

1.6.4 The use of fMRI/EEG/iEEG

Previous studies have shown that EEG-fMRI is a useful method for identifying seizure foci in presumed multifocal seizure in drug-resistant epilepsy (Zijlmans et al., 2007). Using concurrent EEG-fMRI has made localization of regional metabolic changes and ictal activity possible. This non-invasive technique capitalizes both EEG's temporal resolution and fMRI's spatial resolution in seizure localization. However, determining electrophysiological correlation was extremely difficult using EEG-fMRI concurrently. EEG-induced signal distortions in fMRI were also observed. Later, fMRI-induced EEG recording artifacts were removed using high-resolution digitization and post-processing tools (Detre, 2004; Kesavadas & Thomas, 2008). Compared to scalp EEG, the intracranial EEG recording can detect more precise features of regional electrophysiological changes in the brain therefore the iEEG method is regarded as gold-standard for localization of epileptogenic zone. However, the iEEG method has restrictions due to its limited spatial sampling. Simultaneously, functional MRI provides information about the organization and distribution of local and global epileptic brain networks. The combined use of both iEEG and fMRI methods allows analysis of the electrical activity of epileptogenic regions and alterations of neurovascular perfusions occurring as a result of neuronal activity (Vulliemoz et al., 2011). The study conducted by Kucyi et al. (2018) found similar patterns of activity in network connectivity by fMRI analysis and intracranial electrophysiological findings of same brains. Therefore, for the sensitivity and specificity of spatial resolution, intracranial EEG and fMRI have become ideal methods after addressing safety and data quality concerns (Abreu, Leal, & Figueiredo, 2018).

1.6.5 Functional connectivity analysis

The analysis of epileptogenic networks of focal and generalized epilepsies can be characterized by functional connectivity (Gholipour et al., 2022). The functional connectivity metrics are categorized into time-domain and frequency-domain metrics. Time-domain methods include synchronization and causality, such as Granger causality, transfer entropy, and correlations. Frequency-domain analyzes connectivity mechanisms to specific frequency components. The frequency-domain methods include coherence and phase synchronization.

There are two types of functional connectivity measurements. These are directed (causality) and non-directed (coupling). The directed functional connectivity establishes time-lagged cause-effect relationships between signals of brain regions at specific periods. The directed connectivity determines statistical causation by analyzing temporal correlations. Examples include Granger causality, directed and partial-directed coherence, and transfer entropy. In contrast, non-directed connectivity examines statistical associations between brain signals over time without specifying the direction of influence. These include measurements of symmetrical connectivity of spatially distant brain regions, such as correlations and mutual information.

A distinction can be made between model-based and model-free functional connectivity methods in both types i.e., directed and non-directed measurements (Chiarion et al., 2023; khaleghi et al., 2024). Model-based connectivity method selects regions of interest (ROIs) also known as “seeds”. The connections of seeds to the other brain areas are then analyzed by specific metrics, thus generating a connectivity map of the human brain. Model-based methods are classified into cross-correlation analysis, coherence analysis, and statistical parametric mapping. Model-free methods measure brain connectivity without the use of specific models. This method analyses statistical correlations between multi-dimensional neuronal activities. Most functional connectivity measurements use model-based methods based on structural connectivity data (K. Li et al., 2009).

The study of functional connectivity analysis allows us to understand the connectivity between different brain regions by using statistical association between corresponding brain regions by time series fMRI. This stationary FC analysis is also called static FC analysis (Zhou et al., 2023). It is known that human brain interaction is *dynamic* even in a resting state, therefore, FC of brain regions analysed in fMRI data can vary across time. The Dynamic FC elucidates brain network interactions at macroscopic level by investigating time resolved variations in local and global connectivity (Omidvarnia et al., 2016). Various methods are used in dynamic FC which has been summarized into two categories i.e., sliding window method and conceptually innovative extensions (Preti, Bolton, & Van De Ville, 2017).

Sliding window analysis is the most commonly used method for dynamic functional connectivity analysis to understand the dynamic properties of brain connectivity in studying cognitive functions and neurological disorders (Preti, Bolton, & Van De Ville, 2017). This method analyses dynamic FC between different brain regions using fMRI data, where the correlation between fMRI signals (each divided into set of temporal windows) is calculated by moving each window over time. The correlation between each fMRI signal time series of brain regions is calculated by statistical associations such as Pearson correlation. The estimated correlations in the fMRI data reflect changes in brain network connectivity dynamics (Pedersen et al., 2018; Zhou et al., 2023). Besides being useful, the sliding window method has some limitations, such as improper choice of window length, which might alter the output result by escaping the true frequency of fMRI signals (Preti, Bolton, & Van De Ville, 2017).

The dynamic FC on a spatial scale is defined within the millimeter range. Regional homogeneity (ReHo) is one of several local neuronal functional connectivity methods used to investigate the local synchronization of neuronal activity in specific regions of brain. Sliding window ReHo is the extension of ReHo method. The sw-ReHo method is used for local FC dynamics reflecting intrinsic brain activities. Changes in dynamic FC has been detected in several neuropsychological disorders such as conduct disorder, schizophrenia and Alzheimer's disease. However, the sw-ReHo method has several limitations such as the choice of window size and the step size affecting the temporal resolution (Zhou et al., 2023).

To overcome the limitations of sw-ReHo Omidvarnia et al., (2016) developed the dynamic regional phase synchrony (DRePS) method based on phase synchronization. The phase synchronization of neuronal signals is calculated by mean phase coherence in a time series (Zhou et al., 2023). DRePS is method for assessing instantaneous phase synchrony within high-resolution fMRI voxels at each time point in spatially clustered brain regions (Omidvarnia et al., 2016) by providing more dynamic and temporarily precise view of connectivity changes. The DRePS method has been used for analysis of dynamic FC in brain diseases such as there have been increased fluctuations in local connectivity in neocortical focal epilepsy as compared to healthy individuals. This indicates that DRePS helps us understand changes in local dynamic FC in diseased and healthy brains. For the analysis of dynamic FC in focal epilepsy, DRePS is

a promising method that characterizes changes in FC in the region of interest by estimating fMRI dynamic connectivity at its highest temporal resolution (Pedersen et al., 2017).

Epilepsy is regarded as one of the most common network disorders. Various studies of focal epilepsies have demonstrated alteration in functional connectivity in epileptogenic zone compared to FC outside the epileptogenic zone in epileptic patients (Englot, Konrad, & Morgan, 2016a). Various studies reviewed by Feng et al. (2024) show that there have been changes either increase or decrease in functional connectivity in the epileptogenic hemisphere compared to the normal hemisphere of epileptic patients, and some studies have also observed alteration in FC of epileptic brain compared to normal brain (Cao et al., 2017; Feng et al., 2024; Fu et al., 2021). Studies using DRePS analysis framework have also found an increase in signal variability in local connectivity in neocortical focal epilepsy than in healthy individuals using task-free fMRI method (Pedersen et al., 2017).

This study aims to identify local dynamic functional connectivity patterns in the epileptogenic zone using intracranial EEG recording and functional magnetic resonance imaging in drug-resistant focal epilepsy patients. This will be done by comparing the regions of interest, i.e., iEEG electrode locations, with their homologous hemispheric regions, i.e., normal regions, using the DRePS method. The iEEG data will be used as a locator for epileptogenic zone and fMRI data will be used for connectivity analysis. By integrating iEEG data with fMRI-based connectivity analysis this study will help understand the epilepsy specific network alterations due to seizure activity in the epileptogenic hemisphere compared to normal hemisphere of the brain. Therefore, this will provide critical insights into how epilepsy affects brain network dynamics and contribute to uncovering disease pathology.

Chapter 2 Methods

2.1 Patients

The de-identified dataset (intracranial EEG recordings and fMRI images of people with epilepsy) was retrieved online at https://openneuro.org/datasets/ds003688. The dataset (intracranial EEG recordings and fMRI images) of participants was collected while they watched a short audio-visual film during the recordings, while they were admitted to the University Medical Center Utrecht for diagnostic tests for drug-resistant epilepsy.

2.1.1 fMRI dataset

The fMRI dataset consists of 30 participants and 18 of them participated for iEEG recordings as well and 12 of them underwent fMRI only. Data of 17 out of 63 participants were selected for the research project. These 17 patients underwent both iEEG recordings and fMRI scanning, as given in table 2.1 where the fMRI experiment was conducted about several weeks before the iEEG recordings. The non-invasive fMRI was performed prior to the iEEG as the electrode implants can affect the fMRI data. However, the gap between the modalities does not affect the study outcome as the iEEG locations were only used as a locator of hypothesized epileptogenic regions.

During the fMRI scan participants were asked to watch a short movie composed of scenes from “Pippi on the Run”. This video was carefully edited into 6.5 minutes with alternate blocks of speech and music (30 seconds each), seven music blocks, and six speech blocks to engage brain networks for auditory, linguistic, and musical perception. The video was delivered through a screen via a scanner mirror and audio through earphones. The movie was originally in Swedish, but it was dubbed in Dutch to suit participants.

2.1.1.1 fMRI data acquisition

The Philips Achieva 3 T MRI scanner was used for data acquisition using 3D-PRESTO. The functional brain images were acquired using parameters optimized for rapid, whole-brain imaging. The imaging sequence had a repetition time TR of 22.5 milliseconds and echo time TE of 33.2 milliseconds. For temporal resolution, the time to capture one

complete volume was 608 milliseconds. The flip angle was set to 10 degrees to optimize image contrast. The scan included 40 slices covering the whole brain with a field of view measuring 224 x 256 x 160 millimeters and a voxel size of 4 x 4 x 4 millimeters.

2.1.2 iEEG dataset

The iEEG dataset consists of 51 participants (5-55 years) who were asked to watch the same video used for fMRI. Forty-six of them were implanted with electrocorticography grids, where grids had a 2.3 mm exposed diameter. The interelectrode distance was 10mm between 48 and 128 contact points. High-density ECoG electrodes were additionally implanted in six patients, where its exposed diameter was 1.3 with an inter-electrode distance of 3-4mm between 32, 64, and 128 contact points. Sixteen patients were implanted with stereoencephalography electrodes with 4 and 173 contact points. Electrodes were implanted in the left hemisphere of 45 patients, in the right hemisphere of 9 patients, and in both hemispheres of 3 patients.

The sample size comprises 17 participants who underwent both iEEG and fMRI recordings. The sample size is based on the availability of high-quality multimodal data from a rare clinical population with drug-resistant epilepsy undergoing invasive monitoring and treatment (i.e., surgery). Such datasets are limited due to the ethical and logistical constraints of intracranial recordings, which are only performed when clinically indicated. This is an exploratory study where the comparison of dynamic functional connectivity within the same individual is calculated, i.e., comparing ipsilateral and contralateral coordinates. Therefore, this study has limitations in statistical power, as it is an exploratory rather than a definitive study. Nevertheless, the integration of high-resolution iEEG with dynamic fMRI connectivity metrics provides a rich hypothesis-generating framework that can inform future studies.

***Table* 2-1**

List of data of selected participants who have both iEEG and fMRI imaging for the study. The data was retrieved online along with the iEEG and fMRI data for the study (Berezutskaya et al., 2022).

Participant ID	Gender	Age	Handedness	Language dominance	Language dominance technique	iEEG hemisphere
Sub-07	F	42	R	L	fMRI	L
Sub-09	F	33	R	L	fTCD	L
Sub-13	F	17	L	R	Wada	R
Sub-14	F	18	R	R	Wada	L
Sub-16	M	17	R	L	Wada	L
Sub-18	F	15	R	L	fMRI	L
Sub-22	M	21	R	L	fMRI	L
Sub-24	F	47	R	L	Wada	L
Sub-27	M	15	R	L	fMRI	L
Sub-28	M	21	R	L	fMRI	R
Sub-31	F	13	L	R	Wada	LR
Sub-41	M	7	Originally R, but switched to L	Possibly L	ECS (fMRI inclusive)	L
Sub-45	M	19	R	L	fMRI	L
Sub-46	F	41	L	L	fMRI	L
Sub-51	M	46	R	L	fMRI + fTCD	L
Sub-55	F	23	R	L	Wada	L
Sub-60	M	42	R	L	Wada	L

2.2 fMRI data preprocessing

The preprocessing of fMRI data was performed using fMRIPrep software (Esteban et al., 2018) – and the preprocessing sections below follows the fMRIprep boilerplate terminology.

2.2.1 Functional data preprocessing

For the fMRI data, a reference volume was generated, using a custom methodology of *fMRIPrep*, for use in head motion correction. Head-motion parameters with respect to the BOLD reference (transformation matrices, and six corresponding rotation and translation parameters) are estimated before any spatiotemporal filtering using mcflirt (FSL, (Jenkinson et al., 2002)). The BOLD reference was then co-registered to the T1w reference using mri_coreg (FreeSurfer) followed by flirt (FSL, (Jenkinson & Smith, 2001)) with the boundary-based registration (Greve & Fischl, 2009) cost-function. Co-registration was configured with six degrees of freedom. Several confounding time-series were calculated based on the *preprocessed BOLD*: framewise displacement (FD), DVARS and three region-wise global signals. FD was computed using two formulations following Power (absolute sum of relative motions, (Power et al., 2014)) and Jenkinson (relative root mean square displacement between affines, (Jenkinson et al., 2002)). FD and DVARS are calculated for each functional run, both using their implementations in *Nipype* (following the definitions by (Power et al., 2014)). The three global signals are extracted within the CSF, the WM, and the whole-brain masks. Additionally, a set of physiological regressors were extracted to allow for component-based noise correction (*CompCor*, (Behzadi et al., 2007)). Principal components are estimated after high-pass filtering the *preprocessed BOLD* time-series (using a discrete cosine filter with 128s cut-off). For CompCor, three probabilistic masks (CSF, WM and combined CSF+WM) are generated in anatomical space. The implementation differs from that of Behzadi et al. (2007) in that instead of eroding the masks by 2 pixels on BOLD space, a mask of pixels that likely contain a volume fraction of GM is subtracted from the CompCor masks. This mask is obtained by thresholding the corresponding partial volume map at 0.05, and it ensures components are not extracted from voxels containing a minimal fraction of GM. Finally, these masks are resampled into BOLD space and binarized by thresholding at 0.99 (as in the original implementation). Components are also calculated separately within the WM and CSF masks. For each CompCor decomposition, the *k* components with the largest singular values are retained, such that the retained components' time series are sufficient to explain 50 percent of variance across the nuisance mask (CSF, WM, combined, or temporal). The remaining components are dropped from consideration. The head-

motion estimates calculated in the correction step were also placed within the corresponding confounds file. The confound time series derived from head motion estimates and global signals were expanded by including temporal derivatives and quadratic terms for each (Satterthwaite et al., 2013). Additional nuisance timeseries are calculated by means of principal components analysis of the signal found within a thin band (*crown*) of voxels around the edge of the brain, as proposed by Patriat, Reynolds, and Birn (2017). All resamplings can be performed with *a single interpolation step* by composing all the pertinent transformations (i.e. head-motion transform matrices, susceptibility distortion correction when available, and co-registrations to anatomical and output spaces). Gridded (volumetric) resamplings were performed using nitransforms, configured with cubic B-spline interpolation.

2.2.2 Anatomical data preprocessing

The T1w image for each patient was corrected for intensity non-uniformity (INU) with N4BiasFieldCorrection (Tustison et al., 2010), distributed with ANTs 2.5.1 ((Avants et al., 2008), RRID:SCR_004757), and used as T1w-reference throughout the workflow. The T1w-reference was then skull-stripped with a *Nipype* implementation of the antsBrainExtraction.sh workflow (from ANTs), using OASIS30ANTs as target template. Brain tissue segmentation of cerebrospinal fluid (CSF), white-matter (WM) and gray-matter (GM) was performed on the brain-extracted T1w using fast (FSL (version unknown), RRID:SCR_002823, (Zhang, Brady, & Smith, 2001)). Given the individual-specific nature of this thesis, all data used was in the original T1w space, and not an MNI normalised space.

2.2.2.1 Data filtering

The Compcor-based global signal GS, white matter WM, cerebrospinal fluid CSF, and head movement parameters (six motion parameters) were regressed out (Friston et al., 1996) from pre-processed data using Python Pandas and FSL. The data structure of nine parameters i.e., GS, WM, CSF, trans x, trans y, trans z, rot x, rot y, and rot z was constructed using Python Pandas. FSL_GLM was used to regress out these parameters from fMRIPrep data. FSL_Maths was then used to filter the data between 0.03 and 0.07Hz, with a 3rd-order Butterworth filter, to satisfy the Bedrossian requirements for instantaneous phases analysis.

2.3 DRePS

2.3.1 DRePS function

The dynamic regional phase synchrony analysis method was developed as a dynamic extension of the regional homogeneity ReHo method which is used for a static measure of local connectivity i.e., by finding similarity between a voxel and its neighboring voxel. DRePS calculates the instantaneous phase coherence of a voxel with its neighboring voxels at each time point (Omidvarnia et al., 2016; Pedersen et al., 2017). The illustration of DRePS measurement by (Omidvarnia et al., 2016) is given in figure 2.1. The DRePS of the fMRI data was computed using MATLAB R2024b. The DRePS used in this study first extracted pre-processed 4D BOLD fMRI data. The input data consisted of signals from different voxels of the brain over time. The instantaneous phase of these signals was calculated. A moving cube of 27 voxels including a central target voxel with a size of 4x4x4 mm was defined. Then, the dynamic phase coherence was calculated between the target central voxel and its neighbouring 26 voxels of the scan. This estimated time-varying local connectivity was then represented in a 4D map with the same size as the input 4D fMRI data.

Figure 2-1

Schematic illustration of DRePS measurement.

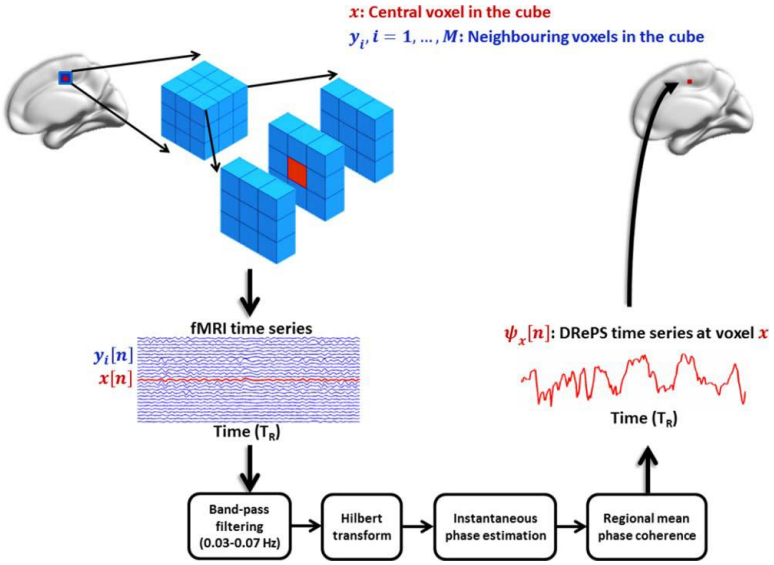

The DRePS measurement is derived from a moving cube of fMRI voxels. This cube consists of a highlighted red central voxel indicated as x surrounded by its 26 neighbouring voxels shown in blue. The DRePS time series is obtained by averaging the instantaneous phase coherence between central voxel x and its adjacent non-zero neighbouring voxels across various time points. This image is the direct copy of DRePS illustration given by Omidvarnia et al. (2016).

2.3.2 DRePS standard deviation

To compare the dynamic functional connectivity of homologous brain regions, first, the standard deviation of the DRePS voxel time series for masked brains was calculated using MATLAB R2024b. The code extracted the fMRI data and applied a brain mask to isolate the voxel time series. The standard deviation of phase synchronization of local connectivity for masked regions was then calculated. The standard deviation estimates temporal variability of local connectivity, such as higher values of standard deviation indicate the presence of more variable voxels over time.

2.3.3 DRePS coordinates

The regions of interest, i.e., the location of iEEG electrodes and their same location in the opposite hemisphere of the same subject were identified, using the closest Euclidian distance calculation of the contralateral hemisphere, at each voxel. The DRePS values of these coordinates of interest (ipsilateral and contralateral) were extracted and the mean and standard deviation of DRePS of the whole brain were also calculated.

2.3.3.1 Paired t-test of ipsilateral and contralateral coordinates

Statistical software Jamovi 2.6.44 was used for statistical calculations. The median value of ipsilateral and contralateral coordinates was calculated. To find the correlations between the regions of interest of each cortical hemisphere the paired t-test statistics were applied where in the t-test result the degree of freedom df is number of intracranial electrodes used for each subject. The paired t-tests were conducted between ipsilateral and contralateral DRePS values. As multiple electrodes were recorded per subject this approach yield multiple within-subject comparisons rather than independent subject level observations. Therefore, standard multiple comparison correction methods such as False Discovery Rate (FDR) designed for independent tests across subjects or voxels are not applied. Instead, the findings are interpreted in context of variability within subjects. This study is electrode level analysis where each intracranial electrode location serves as a unit of comparison. In contrast subject level analysis is performed across subjects which is not applicable in this study as number and locations of electrodes differ in each subject.

Chapter 3 Results

The comparative analysis of ipsilateral and contralateral coordinates shows significant results in 6/17 (35.29 %) of the subjects. A detailed description of the results of each subject of the five subjects with significant DRePS changes, is given below and the results of statistical analysis including significant and non-significant data is given in table 3.1. Individual report of the remaining 11 subjects is found in the appendix.

3.1 Subject 09

Subject 09 is a 33 year old right-handed female with the left hemisphere as language-dominant hemisphere. Functional transcranial Doppler sonography (fTCD) was used to determine the language dominance hemisphere. The iEEG recordings were obtained from left hemisphere located at parietal cortex and hippocampus quadrant, although no high-density grid recordings were used. The comparative analysis of ipsilateral and contralateral coordinates shows a result of $t(68) = -2.24$, $p = 0.029$. This shows that there is a decrease in temporal variability in regions of iEEG electrodes implanted compared to its homologous hemispheric regions.

Figure 3-1

Temporal variations in subject 09.

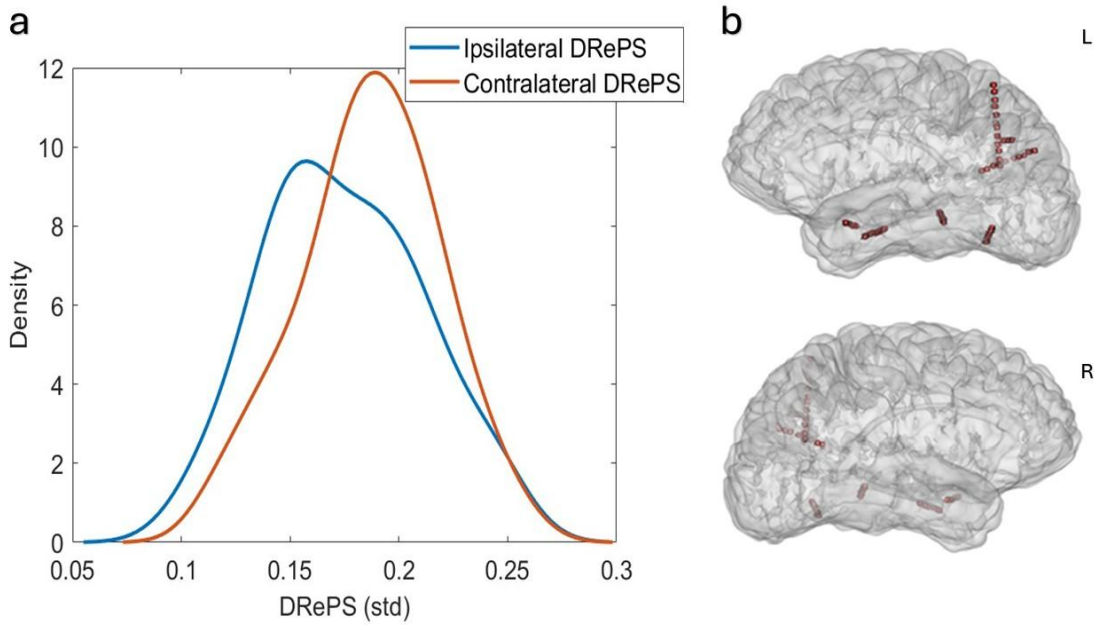

(a) Graph plot of DRePS values of both ipsilateral and contralateral coordinates. The x-axis shows the density of connectivity and y-axis is the value of standard deviation of DRePS of whole brain. (b) The image indicates the locations of iEEG electrodes. L is the left hemisphere and R is right hemisphere of the participant retrieved online from fMRI and iEEG data of participants (Berezutskaya et al., 2022).

3.2 Subject 16

Subject 16 is a 17 year old right-handed male with the language dominance hemisphere identified as left hemisphere. The Wada test was used to identify the language dominance hemisphere. The iEEG recordings were performed at frontal, parietal, temporal, and occipital cortical regions of the left hemisphere of the participant, without the use of high-density grid recordings. The comparative analysis of ipsilateral and contralateral coordinates shows $t(103) = 4.63$, $p < .001$ which indicates a significant result. This means, there is increased temporal variability in affected hemispheric areas compared to its homologous regions.

Figure 3-2

Temporal variations in subject 16.

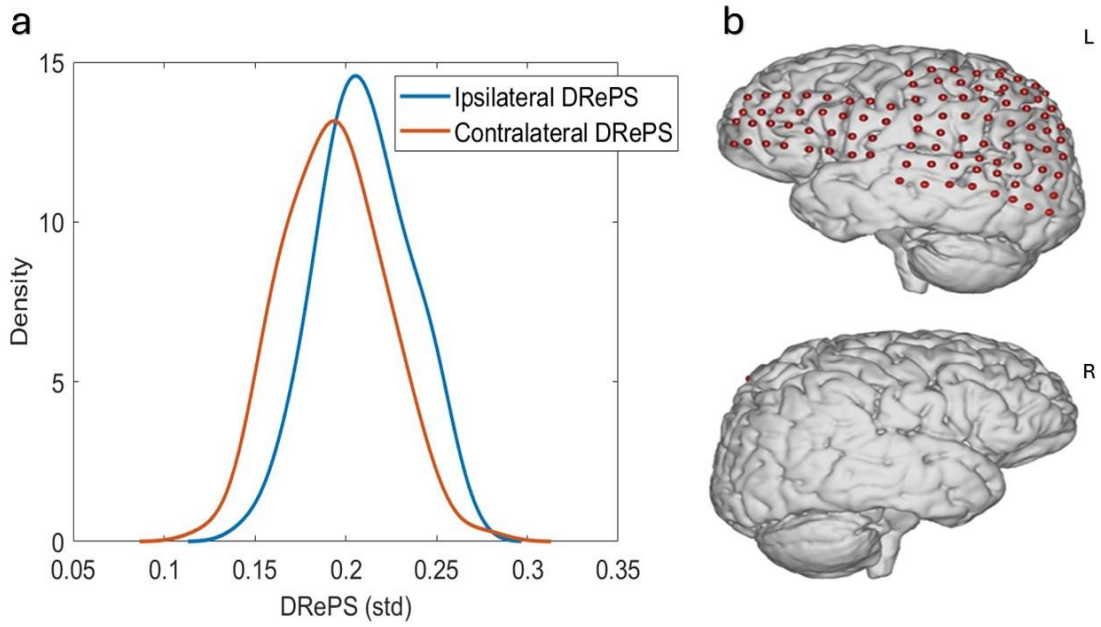

(a) Graph plot of DRePS values of both ipsilateral and contralateral coordinates. The x-axis shows the density of connectivity and y-axis is the value of standard deviation of DRePS of whole brain. (b) The image indicates the locations of iEEG electrodes. L is the left hemisphere and R is right hemisphere of the participant retrieved online from fMRI and iEEG data of participants (Berezutskaya et al., 2022).

3.3 Subject 31

Subject 31 is a 13 year old left-handed female. The Wada test identifies the Participant's right hemisphere as a language-dominant hemisphere. The iEEG electrodes were placed in frontal lobe of left hemisphere and in some parts of frontal and parietal quadrant of right hemisphere.

Figure 3-3

Temporal variations in subject 31.

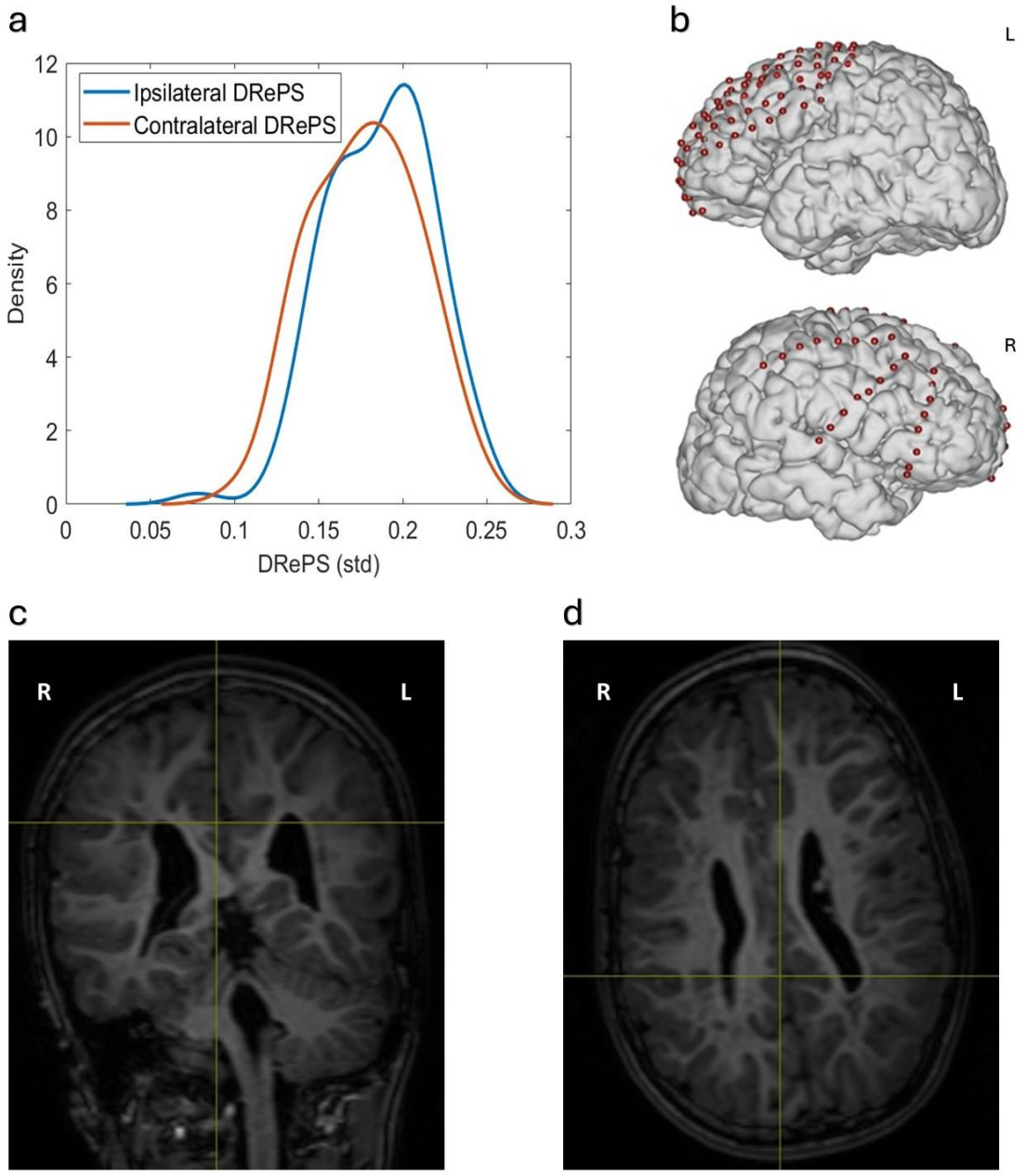

(a) Graph plot of DRePS values of both ipsilateral and contralateral coordinates. The x-axis shows the density of connectivity and y-axis is the value of standard deviation of DRePS of whole brain. (b) The image indicates the locations of iEEG electrodes. L is the left hemisphere and R is right hemisphere of the participant retrieved online from fMRI and iEEG data of the participants (Berezutskaya et al., 2022). (c) Coronal view of brain showing ventricular enlargement in subject 31. (d) Axial view of ventriculomegaly or enlarged ventricular in subject 31. L indicates the left side of the brain and R indicates the right side of the brain.

The comparative analysis of the brain's ipsilateral and contralateral coordinates shows a result of $t(95) = 2.33$, $p = 0.022$. A large scale ventricular abnormality is also present in participant's brain as shown in figure 3.6.

3.4 Subject 45

Subject 45 is a 19 year old right-handed male with left hemisphere identified as language dominant hemisphere. The iEEG recordings were collected from the frontal and temporal lobes of the left hemisphere with some measurements utilizing high density grid electrodes. The comparative statistical analysis of iEEG electrode locations with its homologous regions show a significant of $t(79) = -2.02$, $p = 0.046$. This means there is a decreased temporal variation in ipsilateral regions compared to its homologous areas.

Figure 3-4

Temporal variations in subject 45.

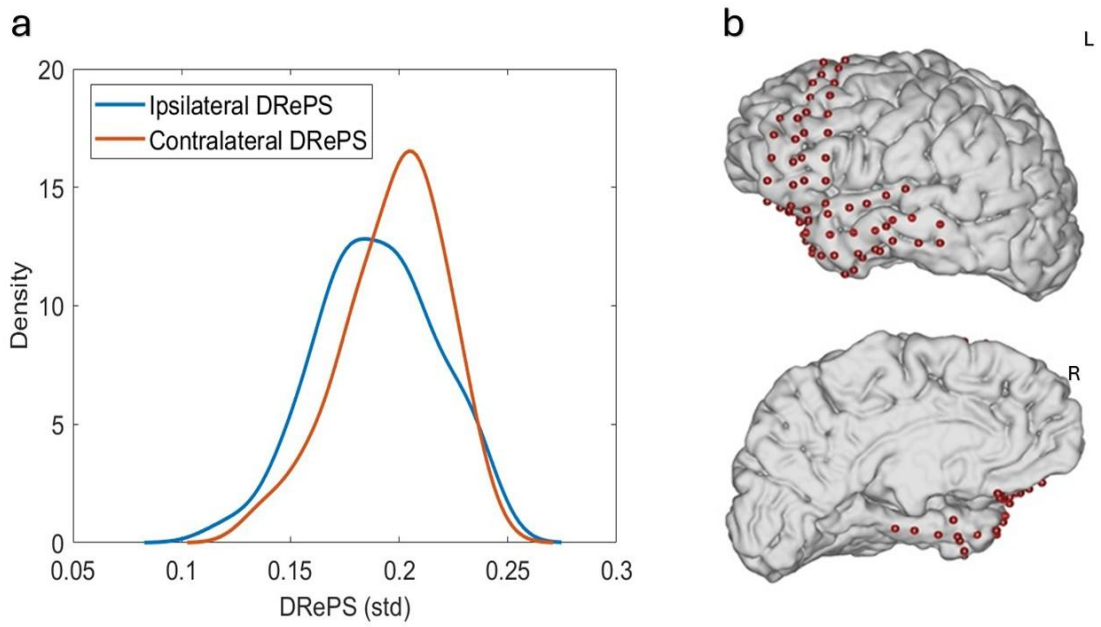

(a) Graph plot of DRePS values of both ipsilateral and contralateral coordinates. The x-axis shows the density of connectivity and y-axis is the value of standard deviation of DRePS of whole brain. (b) The image indicates the locations of iEEG electrodes. L is the left hemisphere and R is right hemisphere of the participant retrieved online from fMRI and iEEG data of participants (Berezutskaya et al., 2022).

3.5 Subject 55

Subject 55 is a 23 year old right handed female who's language dominant hemisphere is left hemisphere determined by Wada test used. The iEEG recordings were performed in the temporal and parietal regions of left hemisphere of participant with no high density

grids used in the recordings. The comparative statistical analysis of regions with iEEG electrodes with its homologous locations show a significant result of $t(95) = -2.24$, $p = 0.017$, which means there is decreased temporal variability in ipsilateral areas compared to its homologous normal regions.

Figure 3-5

Temporal variations in subject 55.

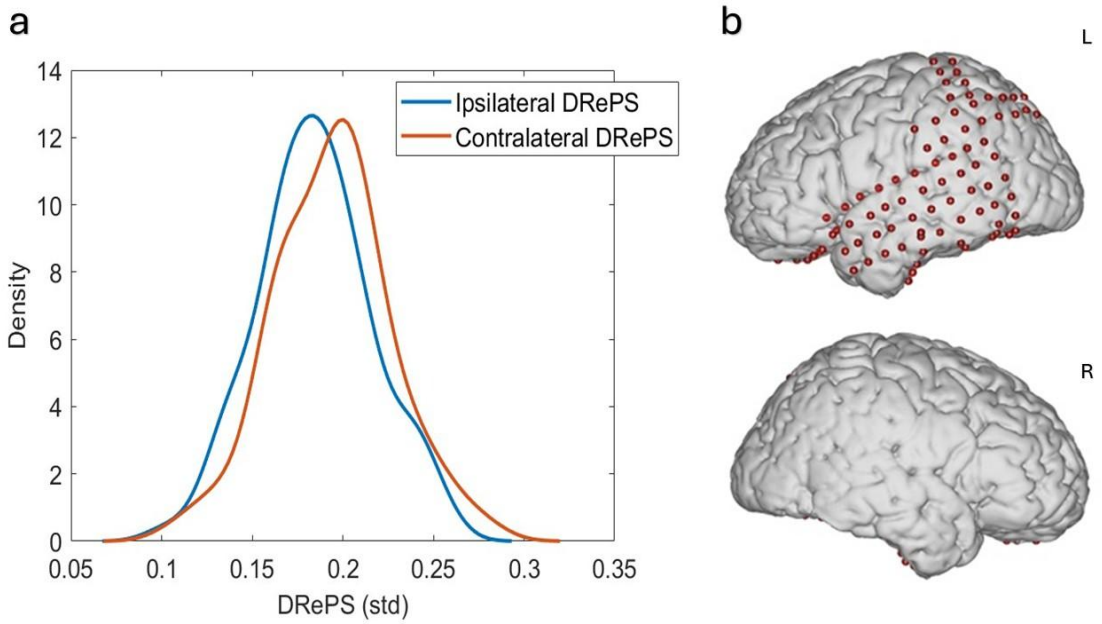

(a) Graph plot of DRePS values of both ipsilateral and contralateral coordinates. The x-axis shows the density of connectivity and y-axis is the value of standard deviation of DRePS of whole brain. (b) The image indicates the locations of iEEG electrodes. L is the left hemisphere and R is right hemisphere of the participant retrieved online from fMRI and iEEG data of participants (Berezutskaya et al., 2022).

3.6 Subject 60

Subject 60 is a 42 year old right handed male, who's language dominance hemisphere is left hemisphere, determined by Wada test. The iEEG measurements were collected from frontal and temporal regions of left hemisphere and some measurements utilized high density grids. The comparative analysis of ipsilateral and contralateral coordinates shows a highly significant result of $t(119) = -4.57$, $p < .001$. This means that there is a decrease in temporal variation in ipsilateral regions as compared to its homologous normal areas.

Figure 3-6

Temporal variations in subject 60.

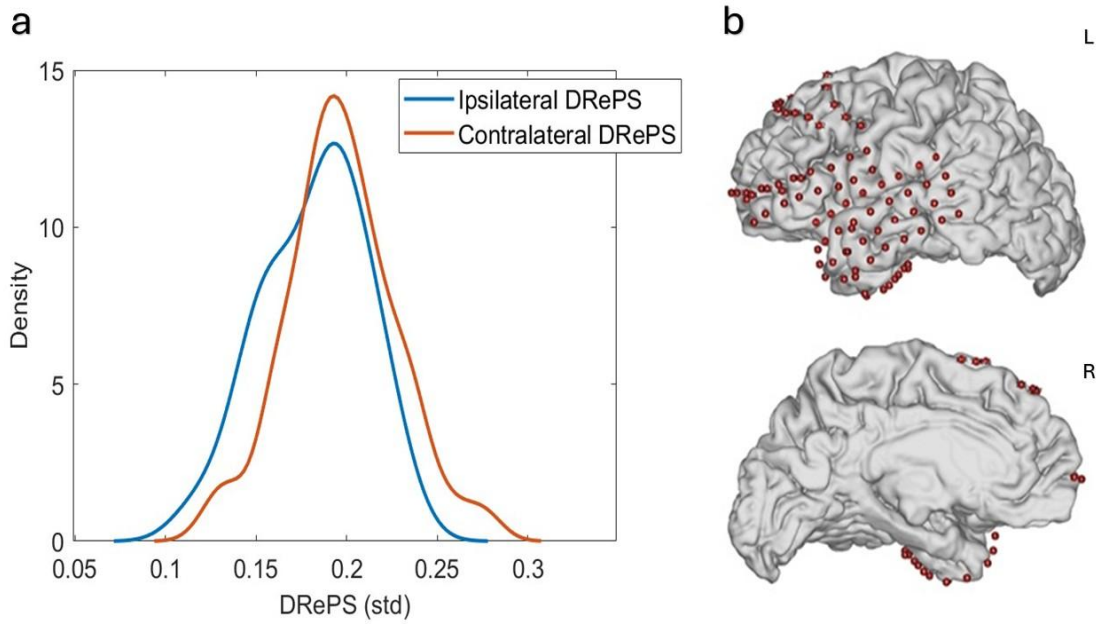

(a) Graph plot of DRePS values of both ipsilateral and contralateral coordinates. The x-axis shows the density of connectivity and y-axis is the value of standard deviation of DRePS of whole brain. (b) The image indicates the locations of iEEG electrodes. L is the left hemisphere and R is right hemisphere of the participant retrieved online from fMRI and iEEG data of participants (Berezutskaya et al., 2022).

Table 3-1

Statistical result of paired t-test of ipsilateral and contralateral coordinates of subjects.

Participant's ID	iEEG hemisphere	DRePS mean	DRePS standard deviation	Degree of freedom (df)	Statistic (t-value)	P-value
Sub-07	L	0.189	0.032	55	-0.523	0.603
Sub-09	L	0.191	0.031	68	-2.24	0.029*
Sub-13	R	0.191	0.031	95	-0.922	0.359
Sub-14	L	0.149	0.036	111	1.19	0.236
Sub-16	L	0.198	0.031	103	4.63	<0.001**
Sub-18	L	0.189	0.031	63	0.0468	0.963
Sub-22	L	0.192	0.030	53	-0.295	0.769
Sub-24	L	0.176	0.035	79	-1.48	0.142
Sub-27	L	0.195	0.030	95	0.613	0.541
Sub-28	R	0.188	0.033	85	1.55	0.126
Sub-31	LR	0.178	0.032	95	2.33	0.022*
Sub-41	L	0.187	0.033	79	-0.872	0.386
Sub-45	L	0.187	0.031	79	-2.02	0.046*
Sub-46	L	0.193	0.031	63	0.411	0.682
Sub-51	L	0.190	0.030	79	0.571	0.570
Sub-55	L	0.192	0.033	95	-2.42	0.017*
Sub-60	L	0.188	0.032	119	-4.57	<0.001**

The table provides information about statistically significant and non-significant results of paired t-test performed on ipsilateral (iEEG hemisphere) and contralateral (normal hemisphere). L indicates the left hemisphere; R indicates the right hemisphere of the brain. A p-value of <0.05 is considered significant, <0.001 is considered a highly significant result while >0.05 is non-significant.

Chapter 4 Discussion

The purpose of this study was to examine individual variation in local dynamic functional connectivity in selected brain regions with iEEG electrodes implanted (presumed epileptogenic) using fMRI data by comparing them to their homologous normal regions in each subject. In this study, the fMRI was performed prior to the use of iEEG as not to get magnetic artifacts from electrodes, which means that it is possible to compute dynamic functional connectivity in regions of interest, which may help predict seizure outcome and identify pathways of seizure propagation in focal epilepsy.

The DRePS method was used to identify temporal variation in these hypothetical epileptogenic regions while watching specific video stimulating language and cognitive abilities. The DRePS method is the updated time-varying version of the sliding-window regional homogeneity ReHo method, which detects dynamic changes in brain connectivity by measuring instantaneous phase coherence within the voxels of the brain (Omidvarnia et al., 2016). The DRePS method is an ideal approach for detecting dynamic changes in the brain by using high temporal resolution (608 mm, per fMRI volume in this study) fMRI data rather than the static ReHo method. This makes it particularly effective for studying rapid neural dynamics and detecting subtle changes associated with seizure activity (Pedersen et al., 2017). The standard deviation of DRePS of these regions shows significant temporal variation compared to contralateral areas in 6 out of 17 subjects (i.e., 35.29%). Therefore, the data result is segregated based on subjects with significant and non-significant temporal variation of ipsilateral coordinates. The significant temporal variation in ipsilateral regions indicates a change in dynamic functional connectivity of these regions (epileptogenic regions) compared to normal homologous regions. This provides information potentially related to the impact of seizure activity on dynamic functional connectivity in the disease hemisphere compared to the normal hemisphere. To further analyse the data, the identification of specific coordinates in the ipsilateral regions with their location that show high levels of temporal variation can help in identifying specific areas of epileptogenic zone related to epileptic lesion in the brain. This study is the basis of studying further the topography of seizure propagation and its effect on global dynamic functional connectivity in refractory focal epilepsy. The global dynamic functional connectivity of focal epilepsy can be performed using whole-

brain functional parcellation method that divides brain into distinct regions or parcels based on their functional characteristics and connectivity patterns (Gholipour et al., 2022).

4.1 Inter-hemispheric alterations in dynamic functional connectivity – clinical implications

This study shows an increase as well as decrease in temporal variability in our cohort, where four subjects display a decrease in temporal variation, and two subjects show increased temporal variability, in ipsilateral coordinates compared to homologous regions. Several studies show a mix of increases and decreases in functional connectivity in epilepsy, and the neurobiological implications of this remains largely unknown. This highlights the network patterns of epilepsy, resulting in heterogenous phenotypic connectivity presumably driven by varying locations of the seizure focus. As the meta-analysis of various individual studies on brain network organization in focal epilepsy suggests that brain network organization is more variable and complex than single studies report (Slinger et al., 2022). This indicates the heterogeneous characteristics of epilepsy, where difference in patterns of functional connectivity is observed in its different types, and changes in functional connectivity also depend on the seizure dynamics and the patient's physiological characteristics. Therefore, the individual study is preferred over group study of refractory focal epilepsy by identifying the alterations in connectivity in different layers of epileptogenic zone and studying patterns of seizure spread in each patient A study conducted by Gupta, Grover, and Abel (2020) using stereo EEG shows epileptogenic cortex shows increased connectivity to regions involving seizure propagation epileptogenic core shows increased local connectivity reflecting hyperexcitable neuronal clusters responsible for seizure initiation. Another study using magnetoencephalography analyzed local functional connectivity in the region of surgical resection by comparing it to their homologous hemispheric regions in refractory epilepsy. Patients with increased functional connectivity in resection regions showed seizure freedom after surgery compared to patients with decreased functional connectivity therefore Englot et al. (2015) suggest that increased local connectivity in resection region could indicate the accurate localization of epileptogenic zone while decreased functional connectivity might indicate incomplete delineation of

epileptogenic zone (Englot et al., 2015). However, investigating dynamic functional connectivity using fMRI data with higher spatial resolution in hypothesized epileptogenic region such as in our study the iEEG electrode locations can help identify epileptogenic zones in those regions, which is different from spatial resolution data as done by previous mentioned research. This can help in under standing pathological studies of focal epilepsy and in identifying network topology and regions of interest for surgical treatment, as the diagnosis and management of refractory focal epilepsy is a challenging task for clinicians due to its heterogeneous characteristics. The use of neuroimaging in combination with physiological data allows us to understand dynamic interactions in brain networks such as a combined study of fMRI with interictal EEG in focal epilepsy has revealed a significant time-dependent relationship between local fMRI connectivity interictal (non-seizure) EEG activity (Omidvarnia et al., 2017).

4.1.1 Decreased temporal variability in ipsilateral hemisphere

A possible explanation of decreased temporal variability in ipsilateral hemisphere comes from subject 09, where the iEEG electrodes were implanted in the parietal and hippocampal quadrants of the left hemisphere given in figure 3.1. The statistical analysis of these regions shows significant temporal variability compared to homologous contralateral regions - a recent study also shows decreased functional connectivity in the hippocampal connectivity in children with temporal lobe epilepsy, and the parietal-temporal lobe of children with temporal lobe epilepsy (Y. Li et al., 2024). In three subjects (subjects 45, 55, and 60), the iEEG electrodes were implanted in the frontal and temporal regions, the temporal and parietal regions, and the frontal and temporal quadrants of the left hemisphere, respectively (see figures 3.4, 3.5, and 3.6 respectively). The ipsilateral coordinates shows a decreased temporal variability compared to contralateral homologous regions. Similarly, research conducted by Klugah-Brown et al. (2019) show a decreased dynamic functional network connectivity in the temporal and spatial domains in epilepsy compared to healthy controls. In a study, decreased inter-hemispheric functional connectivity in benign epilepsy with centrotemporal spikes suggests impaired communication between hemispheres in benign epilepsy with centrotemporal spikes compared to controls (Cao et al., 2017). Another study observed reduced functional connectivity in the temporal cortex of temporal lobe epilepsy compared to healthy controls, suggesting the adaptive mechanism of safeguarding the

contralateral hemisphere by weakening connections within the ipsilateral hemisphere, which can cause generalized seizures in focal epilepsy (Sirin et al., 2020). Therefore, this observation highlights the complex and dynamic nature of neuronal networks in epilepsy, and understanding these changes in functional connectivity can help in the development of treatment for epilepsy.

4.1.2 Increased temporal variability in ipsilateral hemisphere

The highly significant result of paired t-test of ipsilateral and contralateral coordinates in subject 16 shows increased temporal variability in ipsilateral coordinates (that is, frontal, parietal, and occipital regions), indicating increased dynamic functional connectivity compared to the normal hemisphere given in figure 3.2. This is similar to a study conducted for evaluations of functional connectivity in pre-surgical drug-resistant temporal lobe epilepsy in children. The study showed that there was an increase in functional connectivity in temporal lobe of diseased hemisphere compared to normal hemisphere (Grassia et al., 2018). Another study found an increased functional connectivity in the medial temporal lobe and frontal lobe of mesial temporal epilepsy compared to healthy individuals (Liao et al., 2010). The comparative analysis of ipsilateral and contralateral coordinates of subject 31 (see figure 3.3) shows a highly significant result of increased temporal variability in the epileptogenic hemisphere. Ventricular brain abnormality is also visible in the epileptogenic hemisphere of the patient, similar to the results of Sethi, Pedersen, and Jackson (2016), where epileptic patients with polymicrogyric cortex abnormality exhibit changes in functional connectivity. The study compared the functional connectivity of the polymicrogyric cortex with contralateral homologous brain regions, where abnormal brain regions showed stronger and more localized functional connectivity. This suggests that structural brain abnormalities in the epileptogenic hemisphere can influence network connectivity (Sethi, Pedersen, & Jackson, 2016).

4.2 Subjects without temporal variation in ipsilateral coordinates

The DRePS connectivity analysis shows no significant temporal variation in the ipsilateral coordinates compared to homologous contralateral coordinates in subject 13 and 24 (see appendix figure A-2 and A-6 respectively). However, the imaging data of subject 13 shows large-scale ventricular brain abnormality predominantly in the left hemisphere.

The iEEG electrodes were implanted in the right hemisphere of the patient therefore, it is very difficult to find contralateral voxels in the homologous hemisphere. Subject 24, however, had iEEG electrodes implanted in the left hemisphere and a large-scale ventricular abnormality is present predominantly in the left hemisphere. In this case, it is difficult to find ipsilateral voxels. We cannot identify global connectivity alteration by comparing them to healthy individual brains due to lack of data of healthy controls. But another study found changes in global functional connectivity in epileptic patients with polymicrogyric brain abnormalities by comparing them to healthy controls (Sethi, Pedersen, & Jackson, 2016) therefore, there can be alteration in the global functional connectivity of these subjects. The study also requires further analysis of local and global functional connectivity in refractory epileptic patients with brain abnormalities and how brain abnormalities affect the seizure activity in those patients.

The remaining subjects (see appendix figures A-1, A-3, A-4, A-5, A-7, A-8, A-9, A-10, and A-11) show no significant temporal variation in regions with iEEG electrodes compared to their homologous areas. In this study we cannot compare global or local dynamic functional connectivity with healthy controls due to its invasive method iEEG can only be applied to pre-surgical patients with a limited coverage in the cortex. But in theory, it can be hypothesized that systemic focal epilepsy might cause changes in dynamic functional connectivity of both hemispheres due to disease progression therefore we cannot find significant variation in the ipsilateral regions (i.e., epileptogenic zone) compared to the normal hemisphere. As several studies showed that altered functional connectivity in prolonged epilepsy was observed not only in the seizure onset lobe but also extends to broader networks like bilateral attention network, default network mode, and frontoparietal network in several types of pediatric focal epilepsy (Cao et al., 2017; Fang et al., 2017; He et al., 2020; Ibrahim et al., 2014; McGinnity et al., 2017; Morgan et al., 2015; Shamshiri et al., 2017; Sirin et al., 2020; Xiao et al., 2015). Focal epilepsies have been thought of as a regional brain disorder, however, various studies have provided evidence of widespread disruption that extend beyond the epileptogenic zone (Englot, Konrad, & Morgan, 2016b). Another study of resting state MEG of focal epilepsy and control individuals reveals a decrease in widespread global functional connectivity in focal epileptic patients reflecting the long-term effects of recurrent seizures (Englot et al., 2015). Therefore Feng et al. (2024) proposed a two-step model

for how focal epilepsy can evolve to cause widespread disruptions in neural network connectivity over time. The first step involves focal seizure causing progressive white matter damage radiating outwards from seizure focus. The second step includes broader systemic factors progressively increasing the effects causing repeated global insults such as generalized seizures and effects of anti-seizure medications (ASMs), resulting in structural connectivity changes that often affect structural pathways like bilateral cingulum and corpus callosum. Another research conducted by Pedersen et al. (2024) found functional connectivity network alterations in patients with epilepsy after taking antiseizure medications. The functional connectivity pattern also depends on the severity and duration of the disease. Changes in global connectivity in focal epilepsy are linked to neurodegenerative problems, including memory and language disturbances (Englot, Konrad, & Morgan, 2016b). There is a three-layer hypothetical focal-local-global theory proposed that focuses on pathological hubs located at the boundary between local and global brain networks. Normally, an inhibitory ring prevents seizure activity from reaching these hubs. When this inhibition fails, the seizure propagates through the local network, activates the hub, and rapidly spreads across the global network, leading to generalized seizures. Even in the absence of epileptiform abnormalities these hubs can assist in pinpointing the lateralization and localization of the epileptogenic area. According to this focal-local-global hypothesis, removing the pathological hub or disrupting its connections with epileptic focus could reduce or eliminate generalized seizures, as the repeated seizure activity can cause damage to the global network, resulting in loss of integration and potentially leading to cognitive impairments. This highlights the significance of identifying pathological hubs in epilepsy research and preventing global brain damage, causing cognitive defects in epilepsy, as well as pointing towards more effective treatment in epilepsy (Stam, 2016).

Although no significant difference in DRePS values was observed between ipsilateral and contralateral regions in most subjects, this finding reflects a broader pattern of network-level disruption rather than a localized abnormality confined to the epileptogenic zone. Chronic focal epilepsy is increasingly recognized as a disorder of distributed networks with evidence of altered connectivity extending beyond the seizure onset zone. The bilateral symmetry in DRePS may indicate that both hemispheres are affected by long-term seizure activity, neuroplastic changes, or systemic factors such as anti-seizure

medications. These results underscore the importance of considering epilepsy as a dynamic network disorder, highlighting the need for future studies that integrate invasive and non-invasive modalities to map global connectivity alterations more comprehensively.

4.3 Limitations and future directions

This study provides insights into the dynamic functional connectivity in the focal epilepsy; however, due to the heterogeneous nature of epilepsy, the results lack consistency across individuals, limiting the generalizability of findings. The use of invasive EEG has further restricted the sample size, and there is also a lack of data on healthy controls for comparative analysis. Another limitation of this study is lack of post-surgical fMRI data to investigate the effects of surgery in seizure activity. The post-surgical examination can reveal how resection in hypothesized epileptogenic region has affected the brain connectivity dynamics and whether patient has become seizure free. Further research utilizing the use of DRePS for iEEG-fMRI data to investigate local and global dynamic functional connectivity identifying seizure focus points, pathways of spread and modulating centre in drug-resistant focal epilepsy can provide valuable insights to understand patterns of seizure propagation and disease pathology. As DRePS can assist in identifying epileptogenic zone and pathological hubs in focal epilepsy by tacking changes in network alterations and providing temporal perspective on how these networks reorganize. Additionally, incorporating techniques like magnetoencephalography to explore local and global functional connectivity may further enhance our understanding of connectivity alterations in epilepsy. As MEG provides high temporal resolution to detect epileptic spikes and fMRI maps connectivity changes where DRePS can bridge these modalities by capturing instantaneous phase coherence tracking dynamic seizure propagation and assessing epileptogenic zones. The integration of DRePS with iEEG and fMRI data holds a significant promise for improving the clinical management of drug-resistant epilepsy. Traditional surgical planning relies heavily on static imaging, seizure semiology, and interictal/ictal EEG to localize the epileptogenic zone. However, the use of DRePS overlooks the dynamic nature of brain networks involved in seizure initiation and propagation. By capturing the time-varying local synchrony, DRePS provides a novel approach to identifying the pathological network behaviour. In this study, DRePS was used to quantify local phase coherence

variability at electrode locations and their contralateral homologues, offering a dynamic perspective on hemispheric asymmetries and potential pathological hubs. The future application of DRePS on larger datasets can become a valuable addition to the presurgical evaluation toolkit, bridging the gap between network neuroscience and precision neurosurgery.

4.4 Conclusion

The use of fMRI for dynamic functional connectivity analysis of epileptogenic regions based on iEEG electrode locations has provided a significant result of increased and decreased temporal variation in ipsilateral regions of 2 and 4 subjects, respectively, out of a total of 17 subjects with drug-resistant epilepsy, indicating dynamic functional connectivity alterations in these regions. Subjects without any temporal variation in epileptogenic regions might suggest altered global functional connectivity. Overall, the result of this research proposes that iEEG–fMRI analysis using DRePS can provide useful information related to seizure activity in epileptogenic regions of the brain and its impact on global functional connectivity in drug-resistant epilepsy, which may guide surgical planning and outcome.

References

Abreu, R., Leal, A., & Figueiredo, P. (2018). EEG-Informed fMRI: A Review of Data Analysis Methods. *Frontiers in Human Neuroscience, 12*. doi:https://doi.org/10.3389/fnhum.2018.00029

Acharya, U. R., Sree, S. V., Swapna, G., Martis, R. J., & Suri, J. S. (2013). Automated EEG analysis of epilepsy: A review. *Knowledge-Based Systems, 45*, 147-165. doi:https://doi.org/10.1016/j.knosys.2013.02.014

Avants, B. B., Epstein, C. L., Grossman, M., & Gee, J. C. (2008). Symmetric diffeomorphic image registration with cross-correlation: Evaluating automated labeling of elderly and neurodegenerative brain. *Medical Image Analysis, 12*(1), 26-41. doi:https://doi.org/10.1016/j.media.2007.06.004

Bacon, E. J., Jin, C., He, D., Hu, S., Wang, L., Li, H., & Qi, S. (2023). Functional and effective connectivity analysis of drug-resistant epilepsy: a resting-state fMRI analysis. *Frontiers in Human Neuroscience, 17*, 1163111. doi:https://doi.org/10.3389/fnins.2023.1163111.

Bartolomei, F., Lagarde, S., Wendling, F., McGonial, A., Jirsa, V., Guye, M., & Benar, C. (2017). Defining epileptogenic networks: Contribution of SEEG and signal analysis. *Epilepsia, 58*(7), 1131-1147. doi:https://doi.org/10.1111/epi.13791

Behzadi, Y., Restom, K., Liau, J., & Liu, T. T. (2007). A Component Based Noise Correction Method (CompCor) for BOLD and Perfusion Based fMRI. *NeuroImage, 37*(1), 90-101. doi:https://doi.org/10.1016/j.neuroimage.2007.04.042

Beleza, P. (2009). Refractory Epilepsy: A clinically Oreinted Review. *European Neurology, 62*, 65-71. doi:https://doi.org/10.1159/000222775

Berezutskaya, J., Vansteensel, M. J., Aarnoutse, E. J., Freudenburg, Z. V., Piantoni, G., Branco, M. P., & Ramsey, N. F. (2022). Open multimodal iEEG-fMRI dataset from naturalistic stimulation with a short audiovisual film. *Scientific Data, 9*(91). doi:https://doi.org/10.1038/s41597-022-01173-0

Bertram, E. H. (2013). Neuronal circuits in epilepsy: Do they matter? *Experimental Neurology, 244*, 67-74. doi:https://doi.org/10.1016/j.expneurol.2012.01.028

Bromfield, E. B., Cavazos, J. E., & Sirve, J. I. (2006). Basic Mechanisms Underlying Seizures and Epilepsy. In *An Introduction to Epilepsy [Internet]*. Retrieved from https://www.ncbi.nlm.nih.gov/books/NBK2510/

Cao, W., Zhang, Y., Hou, C., Yang, F., Gong, J., Jiang, S., . . . Yao, D. (2017). Abnormal asymmetry in benign epilepsy with unilateral and bilateral centrotemporal spikes: A combined fMRI and DTI study. *Epilepsy Research, 135*, 56-63. doi:https://doi.org/10.1016/j.eplepsyres.2017.06.004

Chang, B. S., & Lowenstein, D. H. (2003). Epilepsy. *New England Journal of Medicine, 349*, 1257-1266. doi:https://doi.org/10.1056/NEJMra022308

Chen, G., Zhang, Z., Wang, M., Geng, Y., Jin, B., & Aung, T. (2021). Update on the Neuroimaging and Electroencephalographic Biomarkers of Epileptogenesis: A Literature Review. *Frontiers in Neurology, 12*. doi:https://doi.org/10.3389/fneur.2021.738658

Chiarion, G., Sparacino, L., Antonacci, Y., Faes, L., & Mesin, L. (2023). Connectivity Analysis in EEG Data: A Tutorial Review of the State of the Art and Emerging Trends. *Bioengineering (Basel, Switzerland), 10*(372). doi:https://doi.org/10.3390/bioengineering10030372

Detre, J. A. (2004). fMRI: Applications in Epilepsy. *Epilepsia, 45*(4), 26-31.

Detre, J. A., Sirven, J. I., Alsop, D. C., O'Connor, M., & French, J. A. (1995). Localization of Subclinical Ictal Activity by Functional Magnetic Resonance Imaging: Correlation with Invasive monitoring. *Annals of Neurology, 38*, 618-624. doi:https://doi.org/10.1002/ana.410380410.

Engel Jr, J. (2014). Approaches to refractory epilepsy. *Annals of Indian Academy of Neurology, 17*, S12-S17. doi:https://doi.org/10.4103/0972-2327.128644

Englot, D. J., Hinkley, L. B., Kort, N. S., Imber, B. S., Mizuiri, D., Honma, S. M., . . . Nagarajan, S. S. (2015). Global and regional functional connectivity maps of neural oscillations in focal epilepsy. *BRAIN, 138*, 2249-2262. doi:https://doi.org/10.1093/brain/awv130

Englot, D. J., Konrad, P. E., & Morgan, V. L. (2016a). Regional and global connectivity disturbances in focal epilepsy, related neurocognitive sequelae, and potential mechanistic underpinnings. *Epilepsia, 57*, 1546-1557. doi:https://doi.org/10.1111/epi.13510

Englot, D. J., Konrad, P. E., & Morgan, V. L. (2016b). Regional and global connectivity disturbances in focal epilepsy, related neurocognitive sequelae, and potential mechanistic underpinnings. *Epilepsia, 57*(10), 1546-1557. doi:10.1111/epi.13510

Esteban, O., Blair, R. W., Markiewicz, C. J., Berleant, S. L., Moodie, C. A., Ma, F., & Isik, A. I. (2018). fMRIPrep 24.0.1. *Software*. doi:10.5281/zenodo.852659

Fang, J., Chen, S., Luo, C., Gong, Q., An, D., & Zhou, Z. (2017). Altered language network in benign childhood epilepsy patients with spikes from non-dominant side: A resting-state fMRI study. *Epilepsy Research, 136*, 109-114. doi:https://doi.org/10.1016/j.eplepsyres.2017.07.020

Feng, X., Piper, R. J., Prentice, F., Clayden, J. D., & Baldeweg, T. (2024). Functional brain connectivity in children with focal epilepsy: A systematic review of functional MRI studies. *Seizure: European Journal of Epilepsy, 117*(164-173). doi:https://doi.org/10.1016/j.seizure.2024.02.021

Fisher, R. S., Boas, W. v. E., Blume, W., Elger, C., Gentone, P., Lee, P., & Engel Jr, J. (2005). Epileptic Seizures and Epilepsy: Definitions Proposed by the International League Against Epilepsy (ILAE) and the International Bureau for Epilepsy (IBE). *Epilepsia, 46*(4), 470-472. doi:https://doi.org/10.1111/j.0013-9580.2005.66104.x

Fisher, R. S., Cross, J. H., D'Souza, C., French, J. A., Haut, S. R., Higurashi, N., . . . Zuberi, S. M. (2017). Instruction manual for the ILAE 2017 operational classification of seizure types. *Epilepsia, 58*(4), 531-542. doi:https://doi.org/10.1111/epi.13671

Friston, K. J. (2011). Functional and Effective Connectivity: A Review. *Brain Connectivity, 1*, 13-36. doi:https://doi.org/10.1089/brain.2011.0008

Friston, K. J., Williams, S., Howard, R., Frackowiak, R. S., & Turner, R. (1996). Movement-related effects in fMRI time-series. *Magnetic Resonance in Medicine, 35*(3), 346-355. doi:https://doi.org/10.1002/mrm.1910350312

Fu, C., Aisikaer, A., Chen, Z., Yu, Q., Yin, J., & Yang, W. (2021). Different Functional Network Connectivity Patterns in Epilepsy: A Rest-State fMRI Study on Mesial Temporal Lobe Epilepsy and Benign Epilepsy With Centrotemporal Spike. *Frontiers in Human Neuroscience, 12*, 1-11. doi:https://doi.org/10.3389/fneur.2021.668856

Gholipour, T., You, X., Stufflebeam, S. M., Loew, M., Koubeissi, M. Z., Morgan, V. L., & Gaillard, W. D. (2022). Common functional connectivity alterations in focal epilepsies identified by machine learning. *Epilepsia, 63*, 629-640. doi:https://doi.org/10.1111/epi.17160

Giourou, E., Stavropoulou-Deli, A., Giannakopoulou, A., Kostopoulos, G. K., & Koutroumanidis, M. (2015). Introduction to Epilepsy and Related Brain Disorders. In N. Voros & C. Antonopoulos (Eds.), *Cyberphysical Systems for Epilepsy and Related Brain Disorders* (pp. 11-38). doi:https://doi.org/10.1007/978-3-319-20049-1_2

Grassia, F., Poliakov, A. V., Poliachik, S. L., Giussani, C., Novotny Jr, E. J., Ojemann, J. G., & Hauptman, J. S. (2018). Changes in resting-state connectivity in pediatric temporal lobe epilepsy. *Journal of Neurosurgery, 22*(3), 270-275. doi:https://doi.org/10.3171/2018.3.PEDS17701

Greve, D. N., & Fischl, B. (2009). Accurate and robust brain image alignment using boundary-based registration. *NeuroImage, 48*, 63-72. doi:https://doi.org/10.1016/j.neuroimage.2009.06.060

Gupta, K., Grover, P., & Abel, T. J. (2020). Current Conceptual Understanding of the Epileptogenic Network From Stereoelectroencephalography-Based Connectivity Inferences. *Frontiers in Neurology, 11*, 569699. doi:https://doi.org/10.3389/fneur.2020.569699

Guye, M., Bartolomei, F., & Ranjeva, J.-P. (2008). Imaging structural and functional connectivity: towards a unified definition of human brain organization? *Current*

opinion in Neurology, 21, 393-403. doi:https://doi.org/10.1097/WCO.0b013e3283065cfb

He, W., Liu, H., Liu, Z., & Wu, Q. (2020). Electrical status epilepticus in sleep affects intrinsically connected networks in patients with benign childhood epilepsy with centrotemporal spikes. *Epilepsy and Behavior, 106*, 107032. doi:https://doi.org/10.1016/j.yebeh.2020.107032.

Health Research Council of New Zealand. Defining Maori epilepsy burden and developing an approach for future research. Retrieved from https://www.hrc.govt.nz/resources/research-repository/defining-maori-epilepsy-burden-and-developing-approach-future

Ibrahim, G. M., Morgan, B. R., Lee, W., Smith, M. L., Donner, E. J., Wang, F., . . . Snead, O. C. (2014). Impaired Development of Intrinsic Connectivity Networks in Children with Medically Intractable Localization-Related Epilepsy. *Human Brain Mapping, 35*(11), 5686-5700. doi:https://doi.org/10.1002/hbm.22580

Jenkinson, M., Bannister, P., Brady, M., & Smith, S. (2002). Improved Optimization for the Robust and Accurate Linear Registration and Motion Correction of Brain Images. *NeuroImage, 17*(2), 825-841. doi:https://doi.org/10.1006/nimg.2002.1132

Jenkinson, M., & Smith, S. (2001). A global optimisation method for robust affine registration of brain images. *Medical Image Analysis, 5*(2), 143-156. doi:https://doi.org/10.1016/S1361-8415(01)00036-6

Jobst, B. C., Bartolomei, F., Diehl, B., Frauscher, B., Kahane, P., Minotti, L., . . . Gotman, J. (2020). Intracranial EEG in the 21st Century. *Epilepsy Currents, 20*(4), 180-188. doi:https://doi.org/10.1177/1535759720934852

Kesavadas, C., & Thomas, B. (2008). Clinical applications of functional MRI in epilepsy. *Indian Journal of Radiology and Imaging, 18*(3), 210-217. doi:https://doi.org/10.4103/0971-3026.41829

Kesavadas, C., Thomas, B., Sujesh, S., & Gupta, A. K. (2007). *Functional MRI (fMRI) Study of Cortical Reorganization in Focal Cortical Dysplasia (FCD)*. Paper presented at the Radiological Society of North America 2007 Scientific Assembly and Annual Meeting, Chicago IL. http://archive.rsna.org/2007/5005263.html

khaleghi, N., Hashemi, S., Pievandi, M., Ardabili, S. Z., Behjati, M., Sheykhivand, S., & Danishvar, S. (2024). EEG-based functional connectivity analysis of brain abnormalities: A systematic review study. *Informatics in Medicine Unlocked, 47*. doi:https://doi.org/10.1016/j.imu.2024.101476

Kim, D.-J., & Min, B.-K. (2020). Rich-club in the brain's macrostructure: Insights from graph theoretical analysis. *Computational and Structural Biotechnology, 18*, 1761-1773. doi:https://doi.org/10.1016/j.csbj.2020.06.039

Klugah-Brown, B., Luo, C., He, H., Jiang, S., Armah, G. K., Wu, Y., . . . Yao, D. (2019). Altered Dynamic Functional Network Connectivity in Frontal Lobe Epilepsy. *Brain Topography, 32*, 394-404. doi:https://doi.org/10.1007/s10548-018-0678-z

Kucyi, A., Schrouff, J., Bickel, S., Foster, B. L., Shine, J. M., & Parvizi, J. (2018). Intracranial Electrophysiology Reveals Reproducible Intrinsic Functional Connectivity within Human Brain Networks. *The Journal of Neuroscience, 38*, 4230-4242. doi:https://doi.org/10.1523/JNEUROSCI.0217-18.2018

Lehnertz, K., Brohl, T., & Wrede, R. v. (2023). Epileptic-network-based prediction and control of seizures in humans. *Neurobiology of Disease, 181*, 106098. doi:https://doi.org/10.1016/j.nbd.2023.106098

Li, K., Guo, L., Nie, J., Li, G., & Liu, T. (2009). Review of methods for functional brain connectivity detection using fMRI. *Computerized Medical Imaging and Graphics: the official journal of the Computerized Medical Imaging Society, 33*, 131-139. doi:https://doi.org/10.1016/j.compmedimag.2008.10.011

Li, Y., Ran, Y., Yao, M., & Chen, Q. (2024). Altered static and dynamic functional connectivity of the default mode network across epilepsy subtypes in children: A resting-state fMRI study. *Neurobiology of Disease, 192*, 106425. doi:https://doi.org/10.1016/j.nbd.2024.106425

Liao, W., Zhang, Z., Pan, Z., Mantini, D., Ding, J., Duan, X., . . . Lu, G. (2010). Altered Functional Connectivity and Small-World in Mesial Temporal Lobe Epilepsy. *PLOS one, 5*(1), e8525. doi:https://doi.org/10.1371/journal.pone.0008525

McGinnity, C. J., Smith, A. B., Yaakub, S. N., Gerbase, S. W., Gammerman, A., Tyson, A. L., . . . Pal, D. K. (2017). Decreased functional connectivity within a language subnetwork in benign epilepsy with centrotemporal spikes. *Epilepsia Open, 2*, 214-225. doi:https://doi.org/10.1002/epi4.12051

Morgan, V. L., Conrad, B. N., Abou-Khalil, B., Rogers, B. P., & Kang, H. (2015). Increasing structural atrophy and functional isolation of the temporal lobe with duration of disease in temporal lobe epilepsy. *Epilepsy Research, 110*, 171-178. doi:https://doi.org/10.1016/j.eplepsyres.2014.12.006

Nascimento, F. A., Friedman, D., Peters, J. M., Bensalem-Owen, M. K., Cendes, F., Rampp, S., . . . Beniczky, S. (2023). Focal epilepsies: Update on diagnosis and classification. *The Educational Journal of the International League Against Epilepsy, 25*(1), 1-17. doi:https://doi.org/10.1002/epd2.20045

Neurological Foundation. (2019). A closer look at a condition: Epilepsy. Retrieved from https://neurological.org.nz/news/a-closer-look-at-a-condition-epilepsy/#!

Neuroscience, S. C. f. R. (2015-2025). OpenNeuro Documentation. Retrieved from https://docs.openneuro.org/index.html

Omidvarnia, A., Pedersen, M., Vaughan, D. N., Walz, J. M., Abbott, D. F., Zalesky, A., & Jackson, G. D. (2017). Dynamic Coupling between fMRI Local Connectivity and

Interictal EEG in Focal Epilepsy: A Wavelet Analysis Approach. *Human Brain Mapping, 38*, 5356-5374. doi:https://doi.org/10.1002/hbm.23723

Omidvarnia, A., Pedersen, M., Walz, J. M., Vaughan, D. N., Abbott, D. F., & Jackson, G. D. (2016). Dynamic Regional Phase Synchrony (DRePS): An Instantaneous Measure of Local fMRI Connectivity Within Spatially Clustered Brain Areas. *Human Brain Mapping, 37*, 1970-1985. doi:https://doi.org/10.1002/hbm.23151

Patriat, R., Reynolds, R. C., & Birn, R. M. (2017). An improved model of motion-related signal changes in fMRI. *NeuroImage, 144*, 74-82. doi:https://doi.org/10.1016/j.neuroimage.2016.08.051

Pedersen, M., & Omidvarnia, A. (2016). Further Insight into the Brain's Rich-Club Architecture. *The Journal of Neuroscience, 36*(21), 5675-5676. doi:https://doi.org/10.1523/JNEUROSCI.0754-16.2016

Pedersen, M., Omidvarnia, A., Curwood, E. K., Walz, J. M., Rayner, G., & Jackson, G. D. (2017). The dynamics of functional connectivity in neocortical focal epilepsy. *NeuroImage: Clinical, 15*, 209-214. doi:https://doi.org/10.1016/j.nicl.2017.04.005

Pedersen, M., Omidvarnia, A., Zalesky, A., & Jackson, G. D. (2018). On the relationship between instantaneous phase synchrony and correlation-based sliding windows for time-resolved fMRI connectivity analysis. *NeuroImage, 181*, 85-94. doi:https://doi.org/10.1016/j.neuroimage.2018.06.020

Pedersen, M., Pardoe, H., Mito, R., Sethi, M., Vaughan, D. N., Carney, P. W., & Jackson, G. D. (2024). Brain network changes after the first seizure: an insight into medication response? *Brain Communications, 6*(5), fcae328. doi:https://doi.org/10.1093/braincomms/fcae335

Power, J. D., Mitra, A., Laumann, T. O., Snyder, A. Z., Schlaggar, B. L., & Petersen, S. E. (2014). Methods to detect, characterize, and remove motion artifact in resting state fMRI. *NeuroImage, 84*, 320-341. doi:https://doi.org/10.1016/j.neuroimage.2013.08.048

Preti, M. G., Bolton, T. A. W., & Van De Ville, D. (2017). The dynamic functional connectome: State-of-the-art and perspectives. *NeuroImage, 160*, 41-54. doi:https://doi.org/10.1016/j.neuroimage.2016.12.061

Sakkalis, V. (2011). Review of advanced techniques for the estimation of brain connectivity measured with EEG/MEG. *Computers in Biology and Medicine, 41*, 1110-1117. doi:https://doi.org/10.1016/j.compbiomed.2011.06.020

San-Juan, D., & Rodríguez-Méndez, D. A. (2023). Epilepsy as a disease affecting neural networks: a neurophysiological perspective. *Neurología (English Edition), 38*(2), 114-123. doi:https://doi.org/10.1016/j.nrleng.2020.06.016

Satterthwaite, T. D., Elliott, M. A., Gerraty, R. T., Ruparel, K., Loughead, J., Calkins, M. E., . . . Wolf, D. H. (2013). An improved framework for confound regression and filtering for control of motion artifact in the preprocessing of resting-state

functional connectivity data. *NeuroImage, 64*, 240-256. doi:https://doi.org/10.1016/j.neuroimage.2012.08.052

Scheffer, I. E., Berkovic, S. F., Capovilla, G., Connolly, M. B., French, J., Guilhoto, L., . . . Zuberi, S. M. (2017). ILAE classification of the epilepsies: Position paper of the ILAE Commission for Classification and Terminology. *Epilepsia, 58*, 512-521. doi:https://doi.org/10.1111/epi.13709

Sethi, M., Pedersen, M., & Jackson, G. D. (2016). Polymicrogyric Cortex may Predispose to Seizures via Abnormal Network Topology: An fMRI Connectomics Study. *Epilepsia, 57*(3), e64-e68. doi:https://doi.org/10.1111/epi.13304

Shah, A. K., & Mittal, S. (2014). Invasive electroencephalography monitoring: Indications and presurgical planning. *Annals of Indian Academy of Neurology, 17*, S89-S94. doi:https://doi.org/10.4103/0972-2327.128668

Shamshiri, E. A., Tierney, T. M., Centeno, M., St Pier, K., Pressler, R. M., Sharp, D. J., . . . Carmichael, D. W. (2017). Interictal Activity is an Important Contributor to Abnormal Intrinsic Network Connectivity in Paediatric Focal Epilepsy. *Human Brain Mapping, 38*(1), 221-236. doi:https://doi.org/10.1002/hbm.23356.

Shariff, S., Nouh, H. A., Inshutiyimana, S., Kachouh, C., Abdelwahab, M. M., Nazir, A., . . . Olivier, U. (2024). Advances in understanding the pathogenesis of epilepsy: Unraveling the molecular mechanisms. *Health Science Reports, 7*, e1896. doi:https://doi.org/10.1002/hsr2.1896

Sirin, N. G., Kurt, E., Ulasoglu-Yildiz, C., Kicik, A., Bayram, A., Karaaslan, Z., . . . Gurses, C. (2020). Functional connectivity analysis of patients with temporal lobe epilepsy displaying different ictal propagation patterns. *Epileptic Disorders, 22*, 623-632. doi:https://doi.org/10.1684/epd.2020.1210

Sirven, J. I. (2015). Epilepsy: A Spectrum Disorder. *Cold Spring Harbour Perspective in Medicine, 5*(9), a022848. doi:https://doi.org/10.1101/cshperspect.a022848

Slinger, G., Otte, W. M., Braun, K. P. J., & Diessen, E. v. (2022). An updated systematic review and meta-analysis of brain network organization in focal epilepsy: Looking back and forth *Neuroscience and Biobehavioral Reviews, 132*, 211-223. doi:https://doi.org/10.1016/j.neubiorev.2021.11.028

Smith, S. J. M. (2005). EEG in the diagnosis, classification, and management of patients with epilepsy. *Journal of Neurology, Neurosurgery & Psychiatry, 76*, ii2-ii7. doi:https://doi.org/10.1136/jnnp.2005.069245

Spencer, S. S. (2002). Neural Networks in Human Epilepsy: Evidence of and Implications for Treatment. *Epilepsia, 43*(3), 219-227. doi:https://doi.org/10.1046/j.1528-1157.2002.26901.x

Stafstrom, C. E. (2006). Epilepsy: a review of selected clinical syndromes and advances in basic science. *Journal of Cerebral Blood Flow and Metabolism, 26*(8), 983-1004. doi:https://doi.org/10.1038/sj.jcbfm.9600265

Stafstrom, C. E., & Carmant, L. (2015). Seizures and Epilepsy: An Overview for Neuroscientists. *Cold Spring Harbour Perspective in Medicine, 5*, a022426. doi:https://doi.org/10.1101/cshperspect.a022426

Stam, C. J. (2016). Epilepsy: What can we learn from Modern Network Theories? *Epileptologie, 33*, 38-43.

Tustison, N. J., Avants, B. B., Cook, P. A., Zheng, Y., Egan, A., Yushkevich, P. A., & Gee, J. C. (2010). N4ITK: Improved N3 Bias Correction. *IEEE Transactions on Medical Imaging, 29*(6), 1310-1320. doi:https://doi.org/10.1109/TMI.2010.2046908

van den Heuvel, M. P., & Sporns, O. (2011). Rich-Club Organization of the Human Connectome. *The Journal of Neuroscience, 31*, 15775-15786. doi:https://doi.org/10.1523/JNEUROSCI.3539-11.2011

Vulliemoz, S., Carmichael, D. W., Rosenkranz, K., Diehl, B., Rodinov, R., Walker, M. C., . . . Lemieux, L. (2011). Simultaneous intracranial EEG and fMRI of interictal epileptic discharges in humans. *NeuroImage, 54*, 182-190. doi:https://doi.org/10.1016/j.neuroimage.2010.08.004

World Health Organization. (2024). Epilepsy. In.

Xiao, F., Li, L., An, D., Lei, D., Tang, Y., Yang, T., . . . Zhou, D. (2015). Altered attention networks in benign childhood epilepsy with centrotemporal spikes (BECTS): A resting-state fMRI study. *Epilepsy and Behavior, 45*, 234-241. doi:https://doi.org/10.1016/j.yebeh.2015.01.016

Zhang, Y., Brady, M., & Smith, S. (2001). Segmentation of brain MR images through a hidden Markov random field model and the expectation-maximization algorithm. *IEEE Transactions on Medical Imaging, 20*(1), 45-57. doi:https://doi.org/10.1109/42.906424

Zhou, J., Zhu, H., Wang, J., & Sun, J. (2023). Dynamic Characteristics of Local Functional Connectivity Revealed by Dynamic Regional Phase Synchrony. *IEEE TRANSACTIONS ON NEURAL SYSTEMS AND REHABILITATION ENGINEERING, 31*, 2507-2517. doi:https://doi.org/10.1109/TNSRE.2023.3276896

Zijlmans, M., Huiskamp, G., Hersevoort, M., Seppenwoolde, J.-H., Huffelen, A. C. v., & Leijten, F. S. S. (2007). EEG-fMRI in the preoperative work-up for epilepsy surgery. *Brain 130*, 2343-2353. doi:https://doi.org/10.1093/brain/awm141

Appendix

Subjects with non-significant temporal variation in ipsilateral brain regions compared to contralateral normal regions.

Subject 07

Subject 07 is a 42-year-old female suffering from refractory epilepsy. The participant is right-handed, but her language dominance hemisphere is the left hemisphere. The iEEG electrodes were implanted in the left hemisphere. The fMRI technique has been used to determine language dominant hemisphere. The comparative statistical analysis of ipsilateral and contralateral coordinates $t(55) = -0.523$, $p = 0.603$. This means there is no significant temporal variation in ipsilateral regions compared to homologous normal brain areas.

Appendix Figure A- 1

Temporal variation in subject 07.

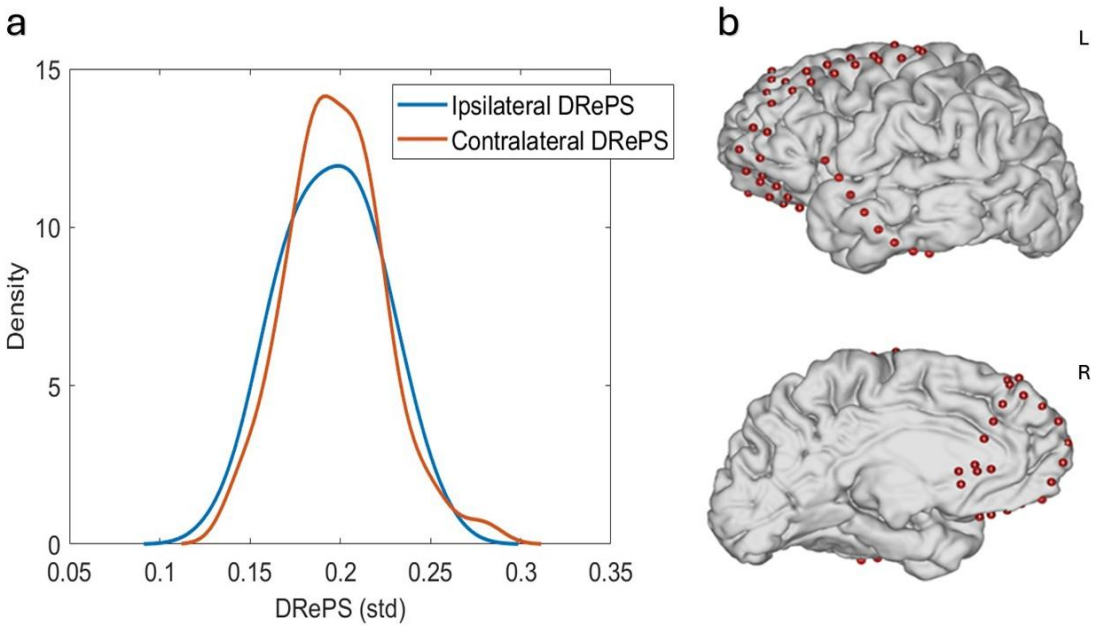

(a) Graph plot of DRePS values of both ipsilateral and contralateral coordinates. The x-axis shows the density of connectivity and y-axis is the value of standard deviation of DRePS of whole brain. (b) The image indicates the locations of iEEG electrodes. L is the left hemisphere and R is right hemisphere of the participant retrieved online from fMRI and iEEG data of participants (Berezutskaya et al., 2022).

Subject 13

Subject 13 is a 17 year old left-handed female with language dominance as right hemisphere, which was determined through Wada test. The iEEG measurements were conducted in the right hemisphere of the brain without the use of high-density grid recordings. The statistical analysis of iEEG locations compared to their homologous regions shows a non-significant result of $t(95) = -0.922$, $p = 0.359$. This means there is no significant temporal variation in ipsilateral regions compared to contralateral coordinates.

Appendix Figure A- 2

Temporal variation in subject 13.

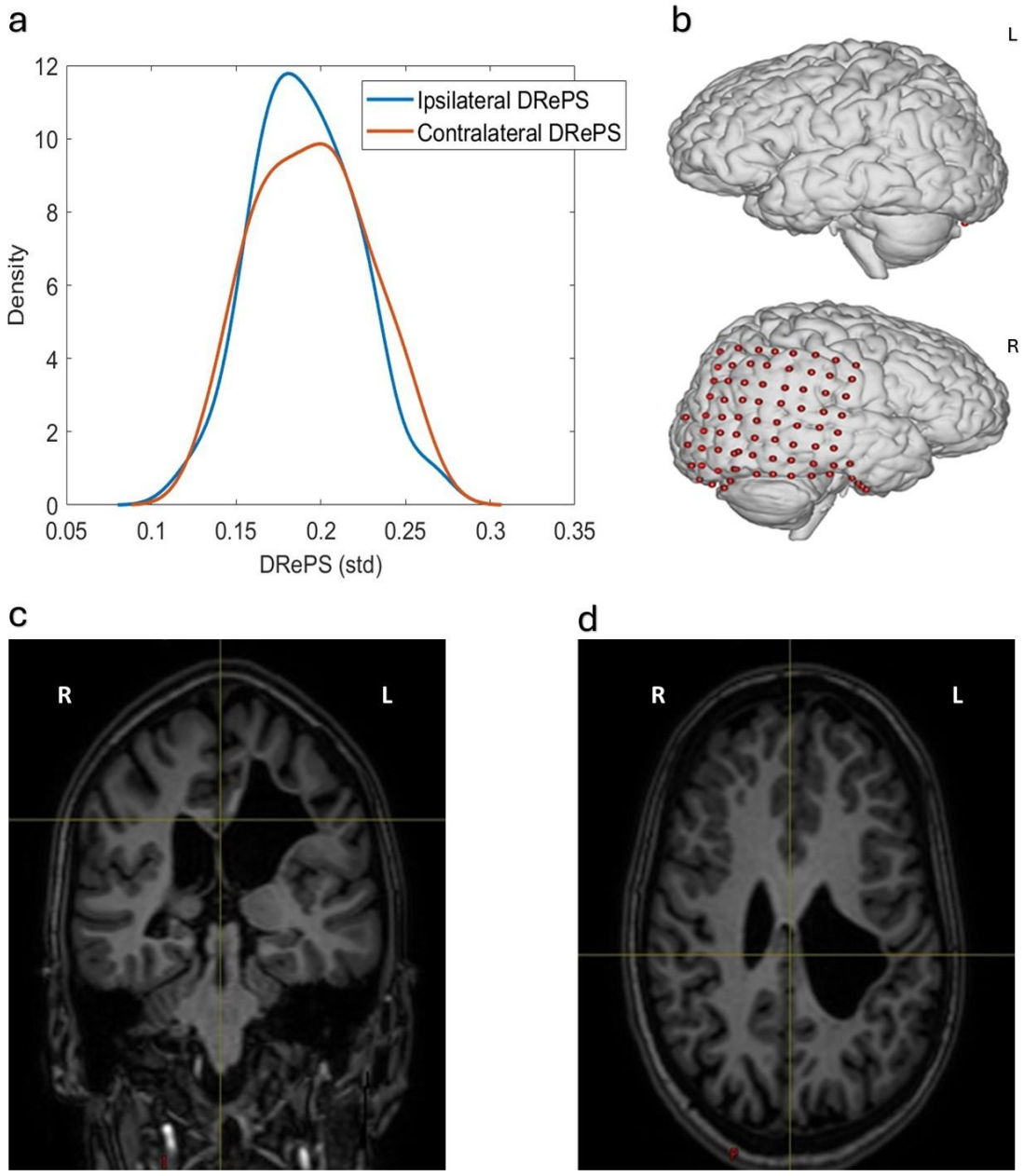

(a) Graph plot of DRePS values of both ipsilateral and contralateral coordinates. The x-axis shows the density of connectivity and y-axis is the value of standard deviation of DRePS of whole brain. (b) The image indicates the locations of iEEG electrodes. L is the left hemisphere and R is right hemisphere of the participant retrieved online from fMRI and iEEG data of participants (Berezutskaya et al., 2022). (c) Coronal view of brain showing ventricular enlargement in subject 31. (d) Axial view of ventriculomegaly in subject 13. L indicates the left side of the brain and R indicates the right side of the brain.

Subject 14

Subject 14 is an 18 year old female who is right handed with language dominant hemisphere as right hemisphere, determined by using Wada test. The iEEG electrodes were localized in left hemisphere of the participant. Some iEEG measurements were utilized by using high density grid. The statistical analysis of iEEG electrode placement regions compared to their homologous regions shows a non-significant result $t(111) = 1.19$, $p = 0.236$. This means there is no significant temporal variation in ipsilateral regions compared to homologous normal brain areas.

Appendix Figure A- 3

Temporal variation in subject 14.

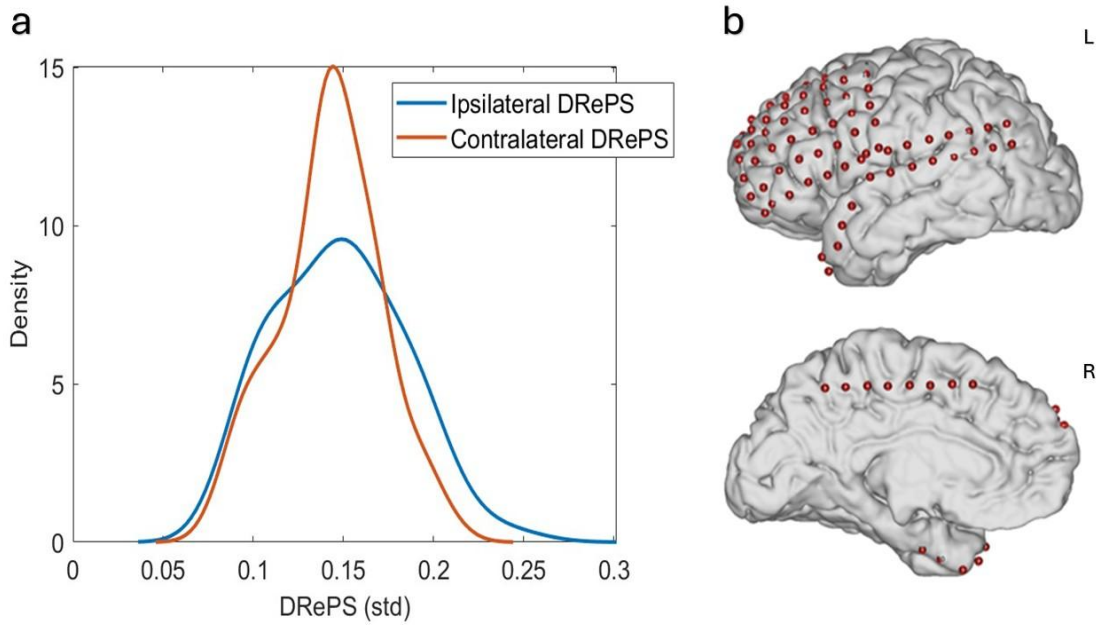

(a) Graph plot of DRePS values of both ipsilateral and contralateral coordinates. The x-axis shows the density of connectivity and y-axis is the value of standard deviation of DRePS of whole brain. (b) The image indicates the locations of iEEG electrodes. L is the left hemisphere and R is right hemisphere of the participant retrieved online from fMRI and iEEG data of participants (Berezutskaya et al., 2022).

Subject 18

Sub 18 is a 15 year old right handed female. The fMRI technique was used to determine the language dominance hemisphere which is left hemisphere. The intracranial EEG recordings were conducted in the left hemisphere of the participant and no high-density grids were utilized. The comparative analysis of ipsilateral and contralateral coordinates

shows no significant result of $t(63) = 0.0468$, $p = 0.963$. This means there is no significant temporal variation in ipsilateral regions compared to homologous normal brain areas.

Appendix Figure A- 4

Temporal variation in subject 18.

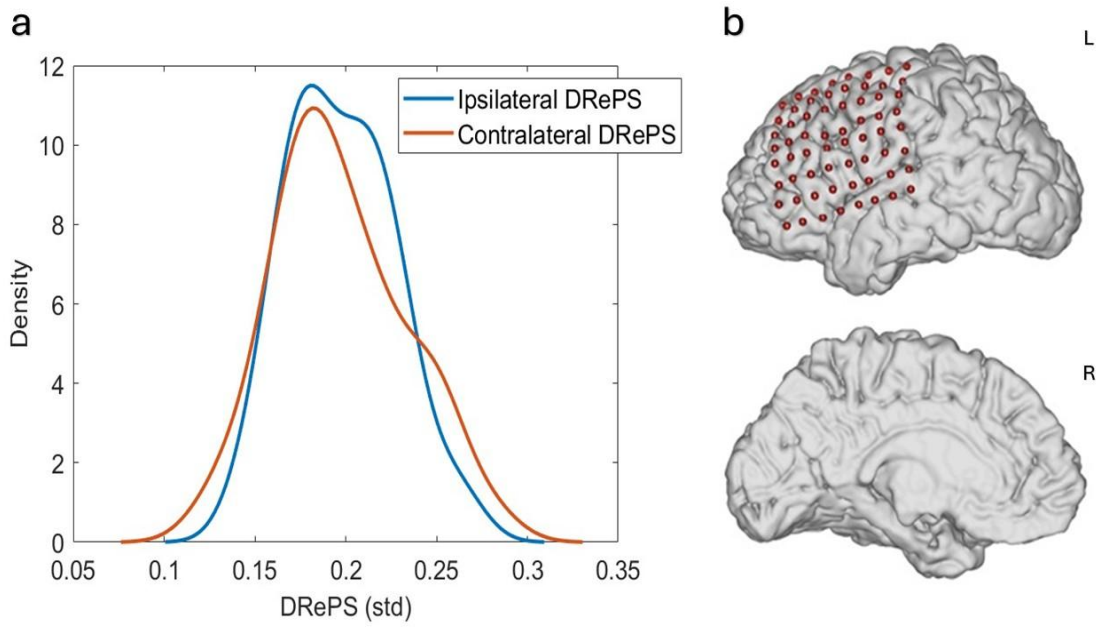

(a) Graph plot of DRePS values of both ipsilateral and contralateral coordinates. The x-axis shows the density of connectivity and y-axis is the value of standard deviation of DRePS of whole brain. (b) The image indicates the locations of iEEG electrodes. L is the left hemisphere and R is right hemisphere of the participant retrieved online from fMRI and iEEG data of participants (Berezutskaya et al., 2022).

Subject 22

Subject 22 is a 21 year right handed male with language dominant hemisphere as left hemisphere. The language dominant hemisphere was determined by fMRI technique. The iEEG electrodes were placed in the left hemisphere of the participant. There were no high-density gird used during the recordings. The comparative analysis of ipsilateral and contralateral coordinates shows no significant result of $t(53) = -0.295$, $p = 0.769$. This means there is no significant temporal variation in ipsilateral regions compared to homologous normal brain areas.

Appendix Figure A- 5

Temporal variation in subject 22.

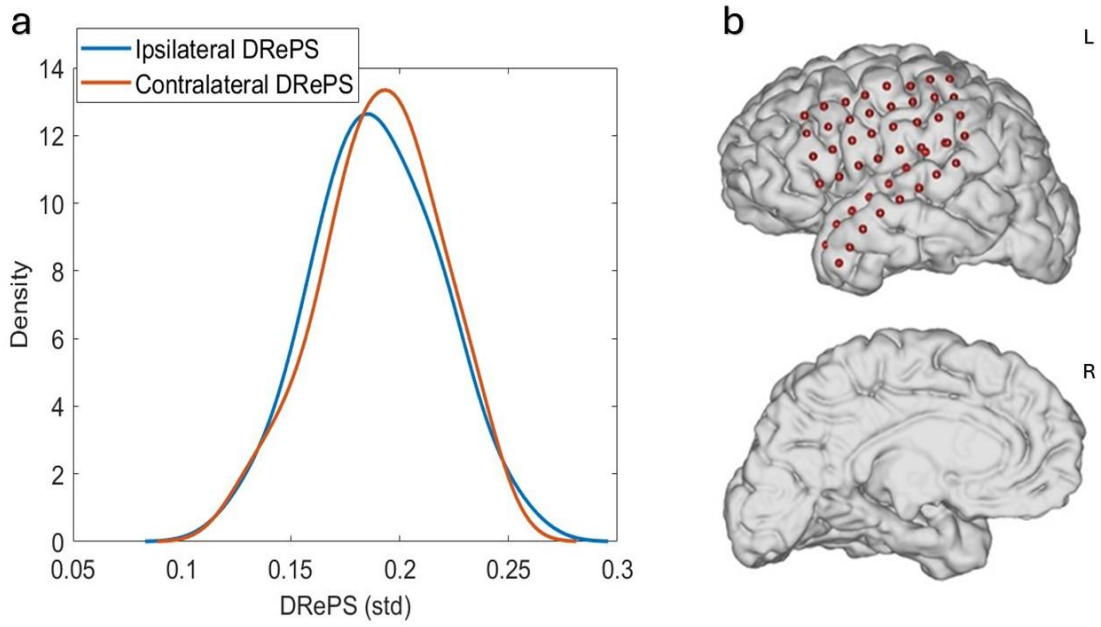

(a) Graph plot of DRePS values of both ipsilateral and contralateral coordinates. The x-axis shows the density of connectivity and y-axis is the value of standard deviation of DRePS of whole brain. (b) The image indicates the locations of iEEG electrodes. L is the left hemisphere and R is right hemisphere of the participant retrieved online from fMRI and iEEG data of participants (Berezutskaya et al., 2022).

Subject 24

Subject 24 is a 47 year old right handed female. The language dominant hemisphere of the participant is left hemisphere determined using Wada test. The intracranial EEG recordings were performed in the left hemisphere and no high-density grid has been used for the recordings. The comparative analysis of ipsilateral and contralateral coordinates shows no significant result of $t(79) = -1.48$, $p = 0.142$. This means there is no significant temporal variation in ipsilateral regions compared to homologous normal brain areas.

Appendix Figure A- 6

Temporal variation in subject 24.

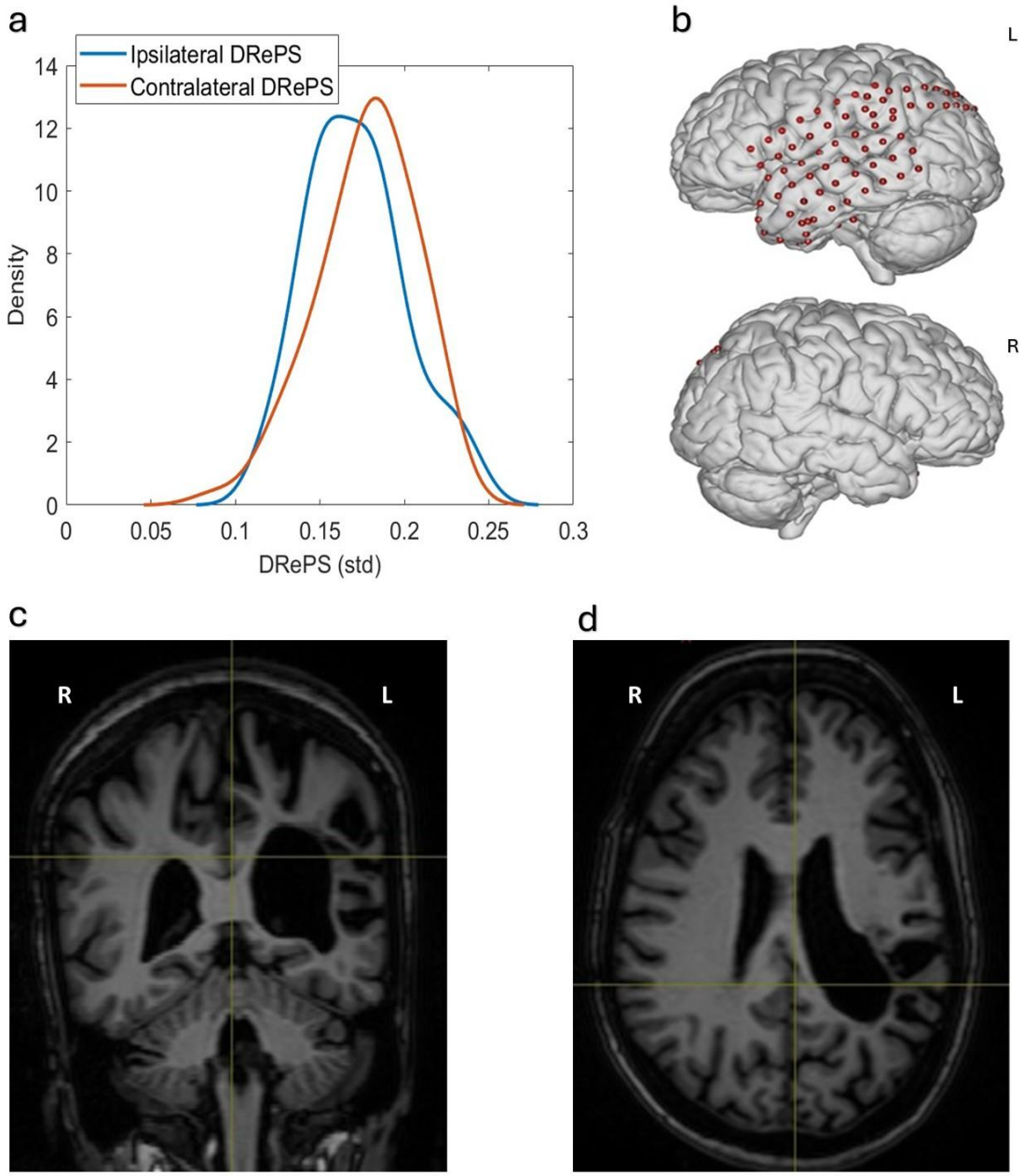

(a) Graph plot of DRePS values of both ipsilateral and contralateral coordinates. The x-axis shows the density of connectivity and y-axis is the value of standard deviation of DRePS of whole brain. (b) The image indicates the locations of iEEG electrodes. L is the left hemisphere and R is right hemisphere of the participant retrieved online from fMRI and iEEG data of participants (Berezutskaya et al., 2022). (c) Coronal view of brain showing ventricular enlargement in subject 31. (d) Axial view of ventriculomegaly in subject 24. L indicates the left side of the brain and R indicates the right side of the brain.

Subject 27

Subject 27 is a 15 year old right handed male with language dominance localized to the left hemisphere as identified through fMRI. The intracranial EEG recordings were also conducted from the left hemisphere and no high density grid recordings were utilized. The comparative analysis of ipsilateral and contralateral coordinates shows no significant result of $t(95) = 0.613$, $p = 0.541$. This means there is no significant temporal variation in ipsilateral regions compared to homologous normal brain areas.

Appendix Figure A- 7

Temporal variation in subject 27.

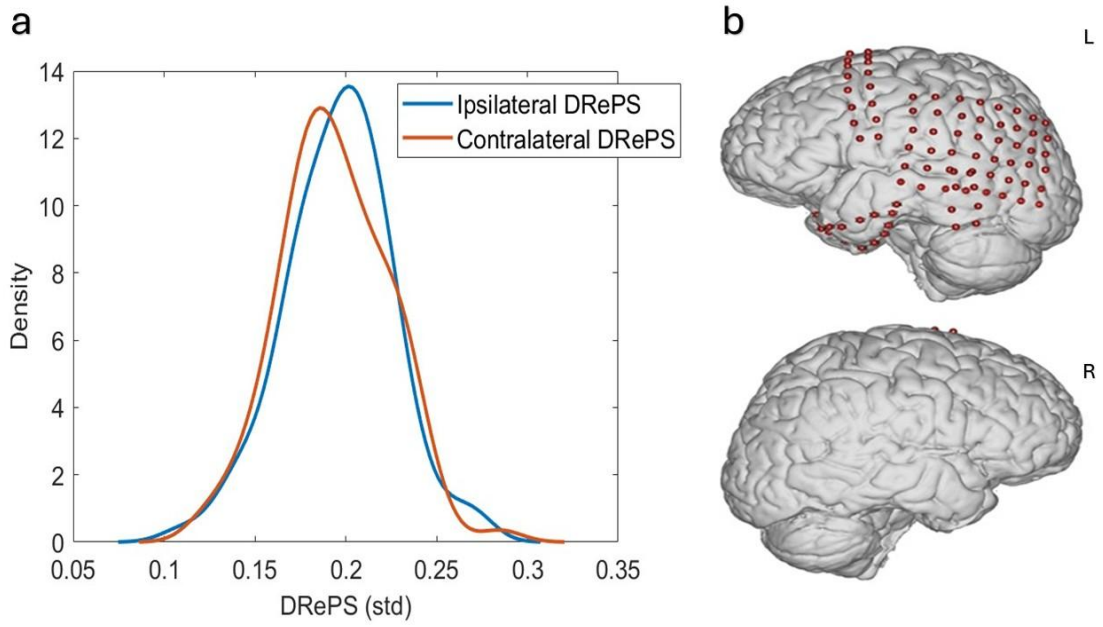

(a) Graph plot of DRePS values of both ipsilateral and contralateral coordinates. The x-axis shows the density of connectivity and y-axis is the value of standard deviation of DRePS of whole brain. (b) The image indicates the locations of iEEG electrodes. L is the left hemisphere and R is right hemisphere of the participant retrieved online from fMRI and iEEG data of participants (Berezutskaya et al., 2022).

Subject 28

Subject 28 is 21 year old right handed male with left hemisphere as language dominant hemisphere. The fMRI technique was used for determining language dominance hemisphere. The iEEG recordings were performed in the right hemisphere of participant's brain. There were no high density grids used for the recordings. The comparative analysis of ipsilateral and contralateral coordinates shows no significant

result of $t(85) = 1.55$, $p = 0.126$. This means there is no significant temporal variation in ipsilateral regions compared to homologous normal brain areas.

Appendix Figure A- 8

Temporal variation in subject 28.

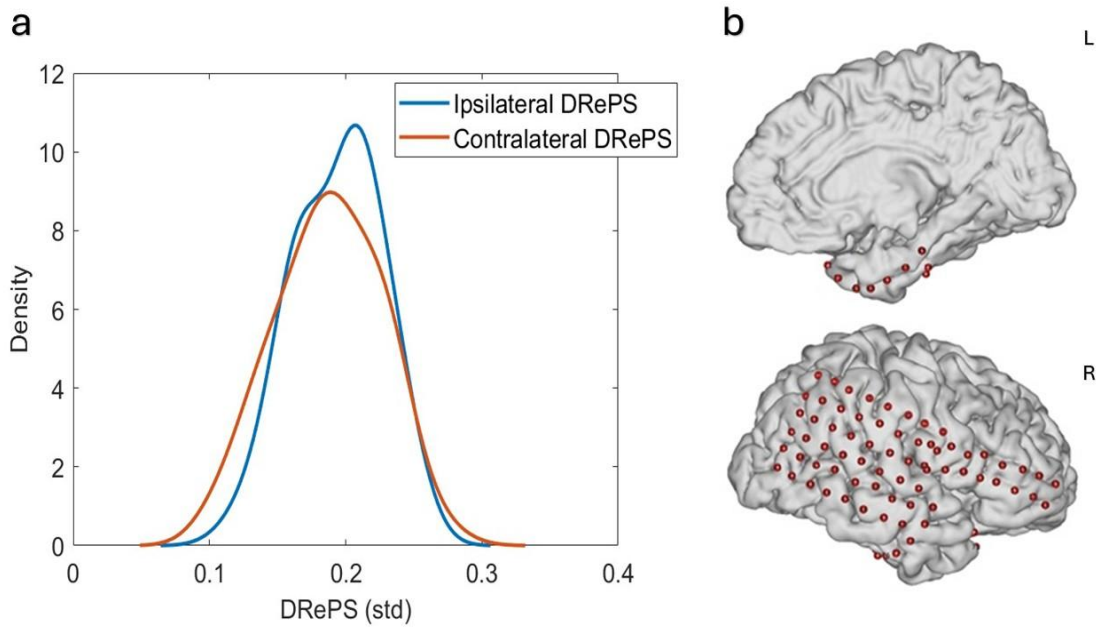

(a) Graph plot of DRePS values of both ipsilateral and contralateral coordinates. The x-axis shows the density of connectivity and y-axis is the value of standard deviation of DRePS of whole brain. (b) The image indicates the locations of iEEG electrodes. L is the left hemisphere and R is right hemisphere of the participant retrieved online from fMRI and iEEG data of participants (Berezutskaya et al., 2022).

Subject 41

Subject 41 is a 7 year old male who was originally right handed but transitioned to left-handedness. Participant's language dominance is possibly located in the left hemisphere, determined using ECS as fMRI results were inconclusive. Intracranial EEG recordings were performed on the left hemisphere, not using high density grids. The comparative analysis of ipsilateral and contralateral coordinates shows no significant result of $t(79) = -0.872$, $p = 0.386$. This means there is no significant temporal variation in ipsilateral regions compared to homologous normal brain areas.

Appendix Figure A- 9

Temporal variation in subject 41.

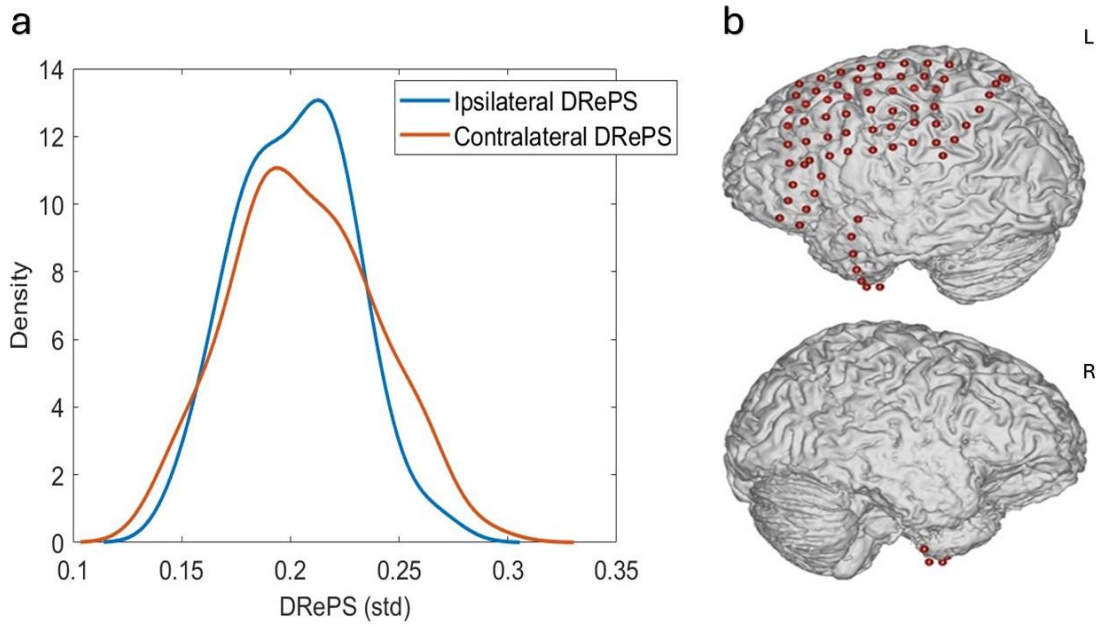

(a) Graph plot of DRePS values of both ipsilateral and contralateral coordinates. The x-axis shows the density of connectivity and y-axis is the value of standard deviation of DRePS of whole brain. (b) The image indicates the locations of iEEG electrodes. L is the left hemisphere and R is right hemisphere of the participant retrieved online from fMRI and iEEG data of participants (Berezutskaya et al., 2022).

Subject 46

Subject 46 is a 41 year old left handed female. The left hemisphere of the participant was identified as language dominant hemisphere using fMRI technique and left hemisphere was used for iEEG recordings with no high density grids. The comparative analysis of ipsilateral and contralateral coordinates shows no significant result of $t(63) = 0.411$, $p = 0.682$. This means there is no significant temporal variation in ipsilateral regions compared to homologous normal brain areas.

Appendix Figure A- 10

Temporal variation in subject 46.

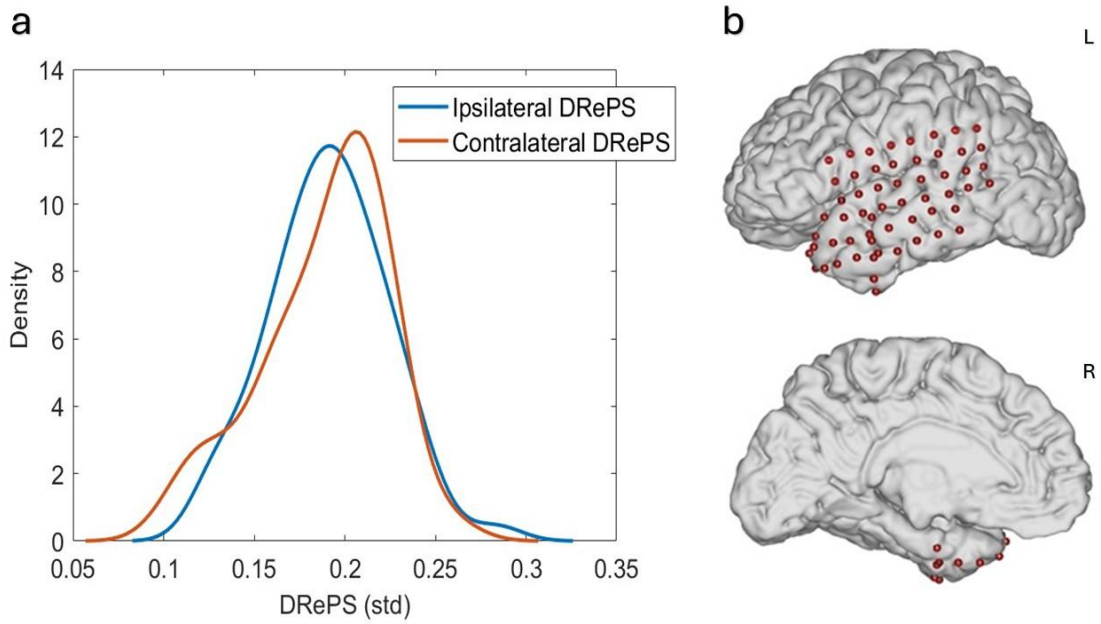

(a) Graph plot of DRePS values of both ipsilateral and contralateral coordinates. The x-axis shows the density of connectivity and y-axis is the value of standard deviation of DRePS of whole brain. (b) The image indicates the locations of iEEG electrodes. L is the left hemisphere and R is right hemisphere of the participant retrieved online from fMRI and iEEG data of participants (Berezutskaya et al., 2022).

Subject 51

Subject 51 is a 46 year old right handed male with left hemisphere as language dominant hemisphere, determined by fMRI and fTCD techniques used. The iEEG electrodes were placed in the left hemisphere without using high density grids. The comparative analysis of ipsilateral and contralateral coordinates shows no significant result of $t(79) = 0.571$, $p = 0.570$. This means there is no significant temporal variation in ipsilateral regions compared to homologous normal brain areas.

Appendix Figure A- 11

Temporal variation in subject 51.

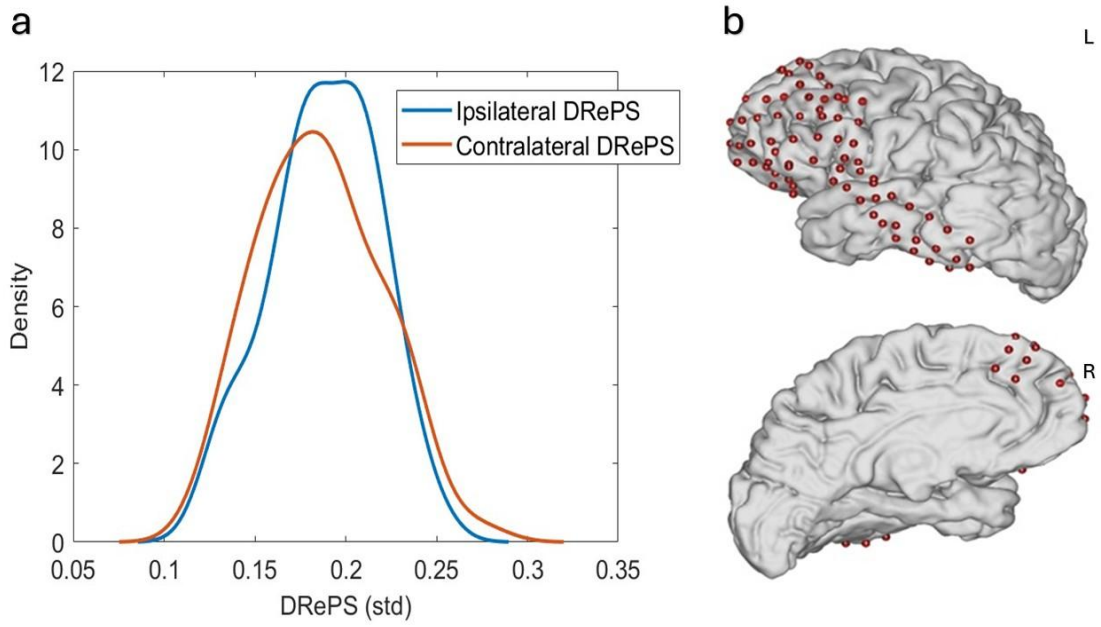

(a) Graph plot of DRePS values of both ipsilateral and contralateral coordinates. The x-axis shows the density of connectivity and y-axis is the value of standard deviation of DRePS of whole brain. (b) The image indicates the locations of iEEG electrodes. L is the left hemisphere and R is right hemisphere of the participant retrieved online from fMRI and iEEG data of participants (Berezutskaya et al., 2022).